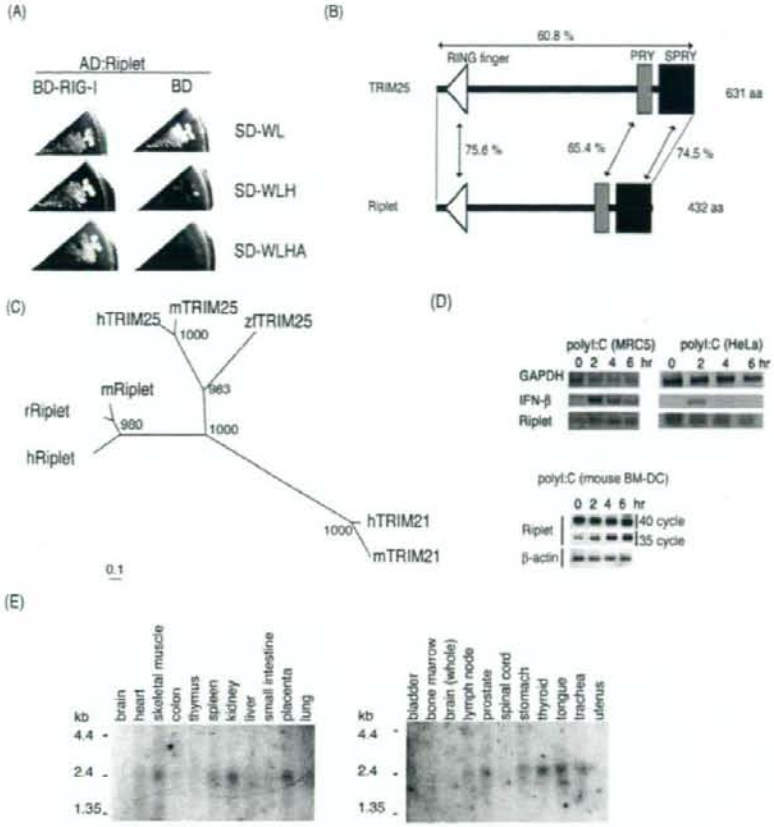

FIGURE 1. **Isolation of Riplet by yeast two-hybrid screening.** *A*, yeast cells carrying both RIG-I and Riplet can grow in selective media (SD-WLH, SD-WLHA), whereas yeast cells carrying RIG-I alone only grow in nonselective media (SD-WL), indicating the physical interaction of RIG-I with Riplet. *B*, human Riplet protein sequence is 60.8% identical to human TRIM25. The RING finger domains and SPRY motifs show higher sequence similarities between the two proteins. *aa*, amino acids. *C*, phylogenetic tree constructed by the Neighbor-Joining method shows that Riplet is similar to TRIM25. *h*, *m*, *r*, or *zf* represent human, mouse, rat, or zebrafish, respectively. The *numbers* on the node are bootstrap probabilities (n = 1000). *D*, HeLa cell, human primary-cultured fibroblast cell, MRC5, or bone marrow-derived mouse dendritic cell (*BM-DC*) were stimulated with poly(I-C) (50 μg/ml) for indicated hours. Total RNA was extracted with TRIzol reagent, and then RT-PCR was carried out using primers shown under "Experimental Procedures." *GAPDH*, glyceraldehyde-3-phosphate dehydrogenase. *E*, Northern blot membranes containing 1 μg of poly(A)$^+$ RNA per lane from human tissues were blotted with human Riplet probe.

tor was added to normalize the final plasmid amount. 48 h after transfection, cells were stimulated with poly(I-C) for 4 h. For VSV infection, 24 h after transfection, cells were infected with VSV at m.o.i. = 1, and cell lysate was prepared after 12 h for reporter gene assays. The degree of gene silencing was confirmed by RT-PCR using RNA extracted from cells 24 h after transfection. PCR primers used for the RT-PCR were Riplet-F3 (ACTGGGAAGTGGACACTAGG) and Riplet-R3 (ACTCATACAGAAGCTTCTCC). siRNAs were purchased from Funakoshi Co., Ltd. (Tokyo Japan), and the siRNA sequences of Riplet siRNA were GACUAUGGACUCUUGUUGUGU (sense) and ACAACAAGAGUCCAUAGUCCU (antisense). Control siRNA sequences were CUGUUGGUUUAGUAAGCCUGU (sense) and AGGCUUACUAAACCAACAGUC (antisense). Another siRNA, Riplet si-1, and control negative siRNA (silencer negative control 1 siRNA, AM4611) were purchased from Applied Biosystems. siRNA sequences were Riplet si-1 GGGAAAGCUUGCCUUCUAUdTdT (sense) and AUAGAAGGCAAGCUUUCCCdTdC (antisense).

Virus Preparation and Infection—VSV Indiana strain and poliovirus were amplified using Vero cells. HEK293 cells were transfected in 24-well plates with plasmid encoding *RIG-I*, Riplet, or no insert. 24 h after transfection, cells were infected with viruses for 24 h, and the titers of virus in culture supernatant were measured by plaque assay using Vero cells. For RNA interference assay, cells were transfected with siRNA with Lipofectamine 2000. 24 h after transfection, cells were infected with viruses at m.o.i. = 0.001 for 18 h, and the titer in culture supernatant were determined by plaque assay.

Immunoprecipitation—HEK293FT cells were transfected in 6-well plates with plasmids encoding FLAG-tagged RIG-I and/or HA-tagged Riplet. The plasmid amounts were normalized by the addition of empty plasmid. 24 h after transfection, cells were lysed with lysis buffer (20 mM Tris-HCl (pH 7.5), 125 mM NaCl, 1 mM EDTA, 10% glycerol, 1% Nonidet P-40, 30 mM NaF, 5 mM Na_3VO_4, 20 mM iodoacetamide, and 2 mM phenylmethylsulfonyl fluoride), and then proteins were immunoprecipitated with rabbit anti-HA polyclonal (Sigma) or anti-FLAG M2 monoclonal antibody (Sigma). The precipitated samples were analyzed by SDS-PAGE and stained with anti-HA (HA1.1) (Covance) or anti-FLAG M2 monoclonal antibody. For ubiquitination assay of RIG-I, the plasmid encoding two multiple HA-tagged ubiquitins was used. HEK293FT cells were transfected with plasmids encoding FLAG-tagged RIG-I, Riplet, or 2× HA-tagged ubiquitin. 24 h after transfection, cells were lysed, and then RIG-I was immunoprecipitated as described above. The samples were analyzed by SDS-PAGE and stained with anti-HA polyclonal antibody (for detection of ubiquitination) or anti-FLAG monoclonal antibody (for detection of RIG-I). Reproducibility was confirmed with additional experiments (see supplemental figures).

Construction of RIG-I 3KA and 5KA Mutant Genes—The C-terminal three or five lysine residues were mutated into alanines (designated as 3KA and 5KA). RIG-I 3KA has K888A, K907A, and K909A, whereas RIG-I 5KA has K849A, K851A,

K888A, K907A, and K909A. The mutant *rig-I* genes were made by PCR-mediated site-directed mutagenesis. The primers used for the PCR were as follows: K907–909A-forward, GTT CAG ACA CTG TAC TCG GCG TGG GCG GAC TTT CAT TTT GAG AAG, and K907–909A-reverse, CTT CTC AAA ATG AAA GTC CGC CCA CGC CGA GTA CAG TGT CTG AAC; K888A-forward, GAC ATT TGA GAT TCC AGT TAT AGC AAT TGA AAG TTT TGT GGT GGA GG, and K888A-reverse, CCT CCA CCA CAA AAC TTT CAA TTG CTA TAA CTG GAA TCT CAA ATG TC; K849–851A-forward, GAG TAG ACC ACA TCC CGC CCA GCG CAG TTT TCA AGT TTT G, and K849–851A-reverse, CAA AAC TTG AAA ACT GCG CTG GCG CGG GAT GTG GTC TAC TC. PCR was carried with Pyrobest *Taq* polymerase, and the obtained clones were sequenced to exclude the clones harboring PCR error. To construct the plasmid-expressing mutant RIG-I protein, the wild-type *RIG-I* gene on pEF-BOS vector was replaced with the mutant *rig-I* gene.

Real Time PCR—Quantitative PCR analyses were carried out using iCycler iQ real time detection system with Platinum SYBR Green qPCR SuperMix-UDG reagent (Invitrogen). Primer sequences for qPCR were as follows: hGAPDH-qF, GAG TCA ACG GAT TTG GTC GT, and hGAPDH-qR, TTG ATT TTG GAG GGA TCT CG; hIFN-β-qF, TGG GAG GAT TCT GCA TTA CC, and hIFN-β-qR, CAG CAT CTG CTG GTT GAA GA; hMx1-qF, ACC ACA GAG GCT CTC AGC AT, and hMx1-qR, CTC AGC TGG TCC TGG ATC TC; and hIFIT-1-qF, GCA GCC AAG TTT TAC CGA AG, and hIFIT-1-qR, CAC CTC AAA TGT GGG CTT TT. Values were expressed as mean relative stimulations, and for a representative experiment from a minimum of three separate experiments, each was performed in triplicate.

RESULTS

RIG-I-binding Proteins—To isolate the proteins that bind to RIG-I, we performed yeast two-hybrid screening using a human lung cDNA library. Using the RIG-I central region (213–601 amino acids), we isolated a clone that encoded a partial ORF of a gene expressed in a dendritic cell line, DC12, whereas the C-terminal region of RIG-I (557–925 amino acids) resulted in the isolation of two cDNA clones, which encoded partial C-terminal regions of ZNF598 and RNF135 (Fig. 1*A* and data not shown). Preliminary expression studies showed that the RNF135 segment affected the RIG-I IFN-β inducing activity, whereas the other two proteins had no effect (data not shown). We confirmed the

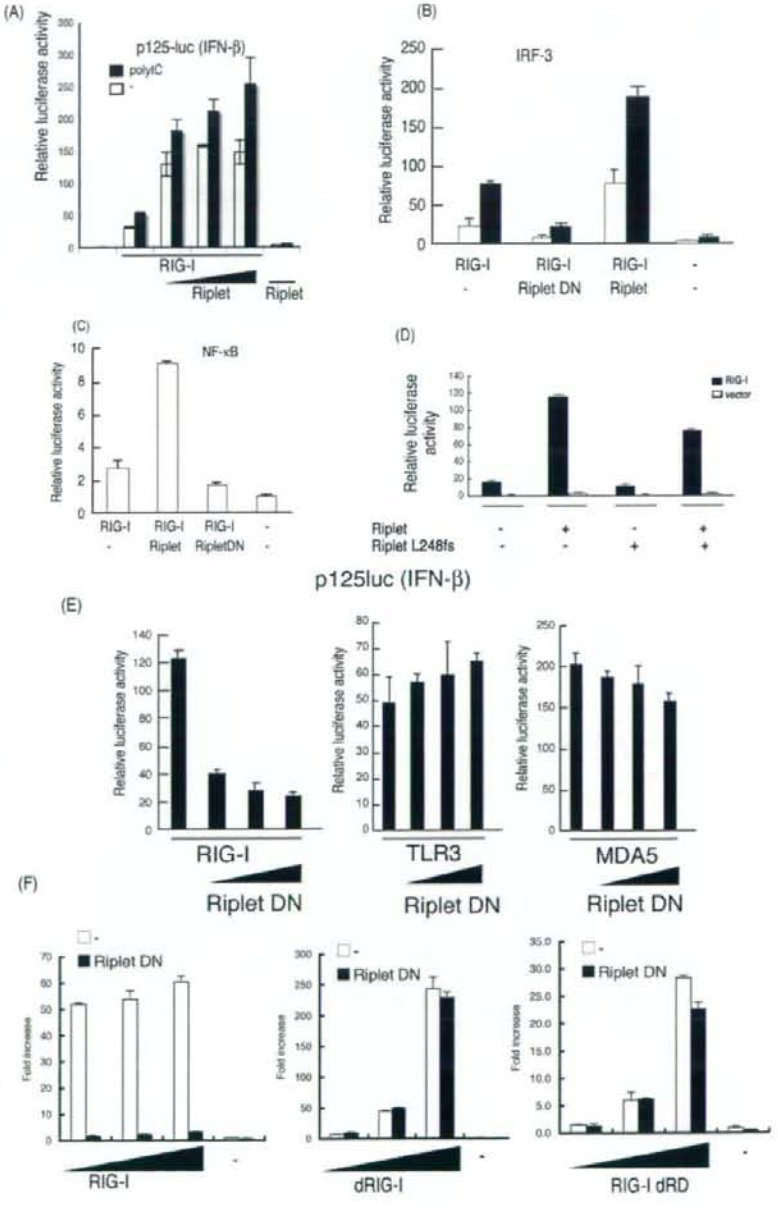

interaction of RIG-I with ZNF598 or RNF135 in HEK293FT cells by immunoprecipitation (data not shown). RNF135 was previously annotated by the genome project and was recently found to be a cause of a genetic disease, neurofibromatosis, although its protein function was unknown. We renamed the protein Riplet (RING finger protein leading to RIG-I activation) based on the following functional analyses. Riplet was most similar to TRIM25 (60.8% sequence homology), in particular between their RING finger domains PRY or SPRY (Fig. 1*B*). Phylogenetic analysis also supported the notion that Riplet was similar to TRIM25 (Fig. 1*C*). Thus, we hypothesized that, like TRIM25, Riplet is a ubiquitin ligase.

Expression of Riplet—RIG-I mRNA is induced by type I IFN or poly(I-C) stimulation in mammalian cells. Unlike RIG-I, however, Riplet mRNA was basally expressed in HeLa and primary-cultured MRC-5 cells irrespective of stimulation (Fig. 1*D* and data not shown). On the other hand, when we treated bone marrow-derived dendritic cells with poly(I-C), the basal level of Riplet mRNA was increased by the stimulation (Fig. 1*D*), suggesting that the regulatory mechanism of Riplet expression somewhat differs among cell types, and that Riplet is expressed before virus infection in some cell types. Next we performed Northern blotting of human tissue RNA. Riplet mRNA was detected as a single band of 2.4 kbp, which is slightly longer than the RNF135 cDNA sequence deposited in GenBank™ (accession number AB470605). Human *RIPLET* is expressed in human skeletal muscle, spleen, kidney, placenta, prostate, stomach, thyroid, and tongue and also weakly expressed in heart thymus, liver, and lung (Fig. 1*E*).

Riplet Enhances RIG-I-mediated IFN-β Induction—At first we characterized the role of Riplet in RIG-I-mediated IFN inducing signaling by reporter gene analyses. When RIG-I was expressed in HEK293 cells, reporter auto-activation was observed even in the absence of exogenous stimulation (Fig. 2*A*) as reported previously (25, 26). Stimulation with poly(I-C) further enhanced the promoter. Co-expression of Riplet with RIG-I potentiated activation of the IFN-β promoter, whereas expression of Riplet alone resulted in only marginal activation (Fig. 2*A*). Detection of endogenous IFN-β mRNA confirmed that Riplet enhanced RIG-I-mediated activation of IFN-β transcription (supplemental Fig. S1). The enhancing role of Riplet in IFN-β promoter activation was also supported by activation of IRF-3 and NF-κB by Riplet (Fig. 2, *B* and *C*). In contrast, expression of a Riplet partial fragment (Riplet-DN) (70–432 amino acids) that lacked the N-terminal RING finger domain reduced promoter activation (Fig. 2*E*). The Riplet-L249fs mutant protein, which was isolated from neurofibromatosis patients (27), did not increase the RIG-I-mediated promoter activation (Fig. 2*D*). These data indicate that Riplet augments RIG-I-mediated IFN-β promoter activation, and that both the RING finger domain and the C-terminal region encoding the SPRY and PRY motifs are important for its function. Riplet (residues 70–432) acted as a dominant-negative form (hereafter called Riplet-DN) (Fig. 2, *E* and *F, left panel*). This functional feature of Riplet-DN was confirmed in Fig. 2, *B* and *C*, and was later confirmed through RIG-I co-precipitation and ubiquitination analyses (see Fig. 5*C* and supplemental Fig. S4*C*). Expression of Riplet-DN did not reduce TLR3 or MDA5 signaling (Fig. 2*E*), suggesting that Riplet-DN is specific for RIG-I signaling. Interestingly, the Riplet-DN only partially suppressed the function of the C-terminal deleted RIG-I (dRD), which is a constitutively active form (Fig. 2*F, right panel*), and RIG-I CARD-like region (dRIG-I)-mediated signaling in high or low dose transfection of dRIG-I was barely inhibited by overexpression of Riplet-DN (Fig. 2*F, center panel*). These data suggest that Riplet requires the RIG-I C-terminal domain (RD) and partial helicase region to activate RIG-I signaling.

Endogenous Riplet Promotes the RIG-I Signaling—We performed Riplet knockdown by siRNA Riplet using Lipofectamine 2000 reagents, instead of FuGENE HD, to reveal the function of endogenous Riplet. Two siRNAs (Riplet siRNA and Riplet si-1) that target different sites of the Riplet mRNA and two control siRNAs were used for knockdown analyses. The two siRNA or control siRNA were co-transfected with HA-tagged Riplet expression vector into HEK293 cells, and after 48 h, cell lysate was prepared and analyzed by Western blotting with anti-HA antibody detecting Riplet. The two siRNAs targeting Riplet abolished exogenously expressed Ripelt-HA, but control siRNA did not (supplemental Fig. S3). Likewise, both Riplet siRNA and Riplet si-1 specifically down-regulate the level of endogenous Riplet mRNA (Fig. 3, *A* and *B*).

Using the siRNA, we examined whether Riplet knockdown reduces RIG-I signaling. As expected, RIG-I-mediated IFN-β promoter activation was reduced by Riplet siRNA or Riplet si-1 compared with control siRNA (Fig. 3, *A* and *B*), indicating that Riplet is required for full activation of the RIG-I signaling. Vesicular stomatitis virus (VSV) is a negative-stranded RNA virus that induces IFN-β production via RIG-I (3). Although the

FIGURE 2. **Riplet enhances IFN-β signaling mediated by RIG-I.** *A*, Riplet enhances the promoter activation by RIG-I. HEK293 cells were transfected with plasmids encoding empty vector, RIG-I (0.1 μg) and Riplet (0.025, 0.05, or 0.1 μg) together with p125-luc (IFN-β promoter) reporter plasmid in 24-well plates. 24 h after transfection, the cells were treated with mock or poly(I-C) (50 μg/ml) for 4 h as described under "Experimental Procedures," and then luciferase activities of cell lysates were measured. *Closed or open boxes* represent poly(I-C) or mock stimulation, respectively. *B*, to examine the activation of IRF-3, RIG-I (0.1 μg), Riplet (0.1 μg), and/or Riplet-DN (0.1 μg),expressing vectors were transfected into HEK293 cells with reporter plasmids, GAL4 fused IRF-3 (0.05 μg), and the p55 UASG-luc reporter gene (0.05 μg), in which luciferase reporter gene is fused downstream of GAL4 protein-binding site, and therefore activated IRF-3 promotes the transcription of luciferase reporter gene. The cells were stimulated with poly(I-C) as described above (34). The total amount of transfected DNA (0.5 μg/well) was kept constant by adding empty vector (pEF-BOS). *C*, HEK293 cells were transfected with RIG-I (0.1 μg), Riplet (0.1 μg), and/or Riplet-DN (0.1 μg) expressing vectors together with the NF-κB reporter plasmid (0.1 μg), and 24 h later, the luciferase activities of cell lysates were measured. *D*, Riplet-L248fs, which lacks the C-terminal region, did not enhance the activation at all. HEK293 cells were transfected with the plasmids expressing wild-type Riplet (0.1 μg) or Riplet-L248fs (0.1 μg) together with RIG-I expressing vector (0.1 μg) and p125-luc reporter (0.1 μg). 24 h after transfection, cell were stimulated with poly(I-C), and the luciferase activities of cell lysates were determined as described above. *E*, RIG-I (0.1 μg), MDA5 (0.1 μg), or TLR3 (0.1 μg) expressing vectors were transfected into HEK293 cells with the plasmid encoding the Riplet-DN fragment (0.1, 0.2, or 0.3 μg) in 24-well plates. After 24 h, the cells were stimulated with 50 μg of poly(I-C) for 4 h, and relative luciferase activities were determined. *F*, Riplet-DN (100 ng) was co-transfected with full-length RIG-I (0, 50, 100, or 200 ng), RIG-I CARD-like region (dRIG-I) (0, 50, 100, or 200 ng), or C-terminal deleted RIG-I (RIG-I dRD) (0, 50, 100, or 200 ng) into HEK293 cells in 24-well plate, and reporter gene assays were carried out.

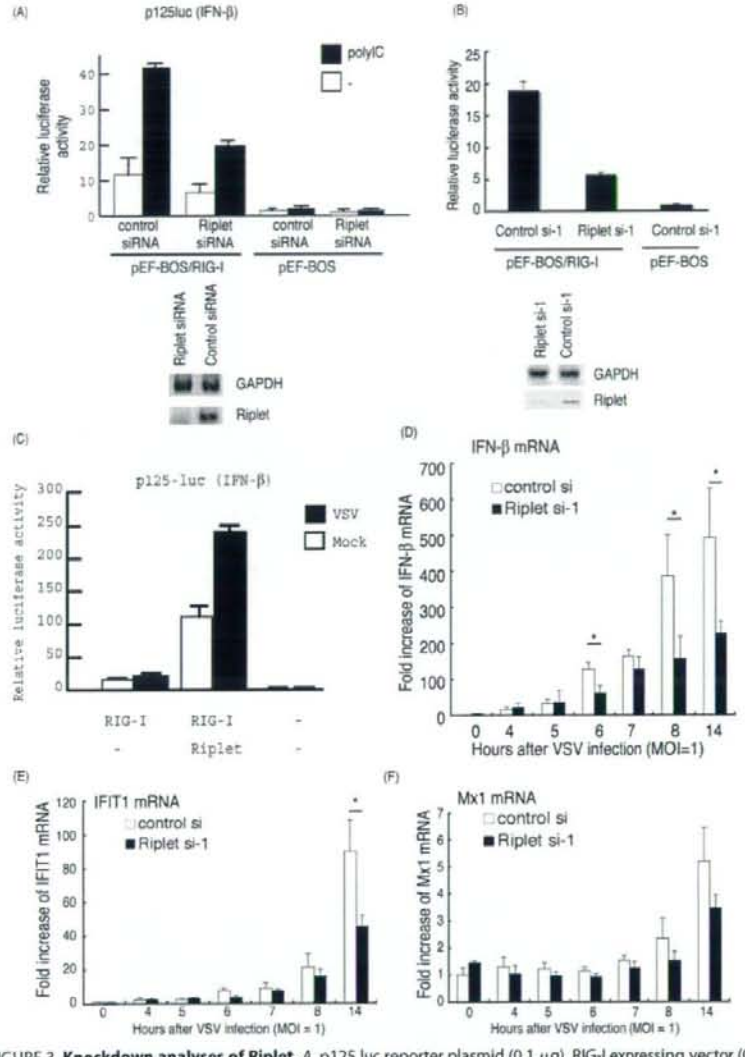

FIGURE 3. **Knockdown analyses of Riplet.** *A*, p125 luc reporter plasmid (0.1 μg), RIG-I expressing vector (0.1 μg), and Riplet siRNA or control siRNA (10 pmol), which were purchased from Funakoshi Co. Ltd., were transfected into HEK293 cells in a 24-well plate with Lipofectamine 2000, and 48 h after transfection, the cells were stimulated with poly(I-C) for 6 h, and the cell lysate was prepared, and luciferase activities were measured. RT-PCR was carried out using total RNA extracted from cells 48 h after transfection. *B*, p125 luc reporter plasmid (0.1 μg), RIG-I expressing vector (0.1 μg), and siRNA, Riplet si-1, or control si-1 (10 pmol), which were purchased from Applied Biosystems, were transfected into HEK293 cells with Lipofectamine 2000. 48 h after transfection, the cells were stimulated with poly(I-C) for 6 h. The cell lysate was prepared, and luciferase activities were measured. RT-PCR was carried out using total RNA extracted from cells 48 h after transfection. *C*, HEK293 cells were transfected with the plasmids expressing RIG-I (0.1 μg) and/or Riplet (0.1 μg) with p125 luc reporter plasmid (0.1 μg) in 24-well plates. After 24 h, the cells were infected with VSV (m.o.i. = 1) for 12 h. The luciferase activities of the cell lysates were measured. Expression of Riplet strongly enhanced IFN-β promoter activation by VSV through RIG-I. *D–F*, siRNA (control si- or Riplet si-1) were transfected into HEK293 cells, and after 48 h, the cells were infected with VSV at m.o.i. = 1. RNA was extracted at the indicated hours, and the quantitative PCR were carried out to detect the expression of IFN-β (*D*), IFIT-1 (*E*), or Mx1 (*F*) mRNA. *, $p < 0.05$. *GAPDH*, glyceraldehyde-3-phosphate dehydrogenase.

IFN-β promoter was only minimally activated by RIG-I in response to VSV (m.o.i. = 1) during the early phase of infection (<12 h), the activity was increased by RIG-I and Riplet (Fig. 3*C*). Riplet was silenced by siRNA and then VSV infected the cells. VSV-derived up-regulation of IFN-β mRNA was started around 6 h post-infection, and Riplet siRNA significantly suppressed the increase of IFN-β mRNA at 6 h (Fig. 3*D*). Because VSV infection is mainly sensed by RIG-I, this is consistent with the notion that Riplet promotes the RIG-I signaling. Other IFN-inducible genes, *IFIT1* and *MX1*, were expressed >8 h post-infection, and their expressions were also suppressed by Riplet siRNA (Fig. 3, *E* and *F*).

Riplet Exerts Protective Activity against Viral Infection—Next we examined the role of Riplet during viral infection. Riplet and/or RIG-I were transiently expressed in the human cells by FuGENE HD reagents, and then the cells were infected with VSV or poliovirus (a positive-stranded RNA virus). The viral titer of the supernatant was determined 24 h post-infection. Under our conditions, expression of RIG-I weakly inhibited VSV propagation. Co-expression of Riplet with RIG-I significantly suppressed VSV replication especially at low m.o.i., whereas Riplet alone did not suppress VSV (Fig. 4, *A* and *B*, *upper panel*). Therefore, a sufficient amount of RIG-I protein is required for Riplet to exert antivirus activity. This requirement of RIG-I is also observed in reporter gene analyses (Fig. 2). Under a similar setting, the antiviral effect of Riplet was marginally observed against poliovirus, which induces IFN-β largely via MDA5 (Fig. 4*B*, *lower panel*). To assess the importance of endogenous Riplet for antivirus effect of human cells, Riplet knockdown cells were infected with viruses. In Riplet knockdown cells, the VSV titer was consistently increased compared with the control ($p < 0.05$) (Fig. 4*C*, *left panel*). In addition, infection of Riplet knockdown cells with poliovirus resulted in only a slight increase in the poliovirus titer compared with the control ($p > 0.05$) (Fig. 4*C*, *right panel*). Because poliovirus is mainly recognized by MDA5 but not RIG-I, this marginal effect of Riplet on poliovirus infection was within expectation (3, 28).

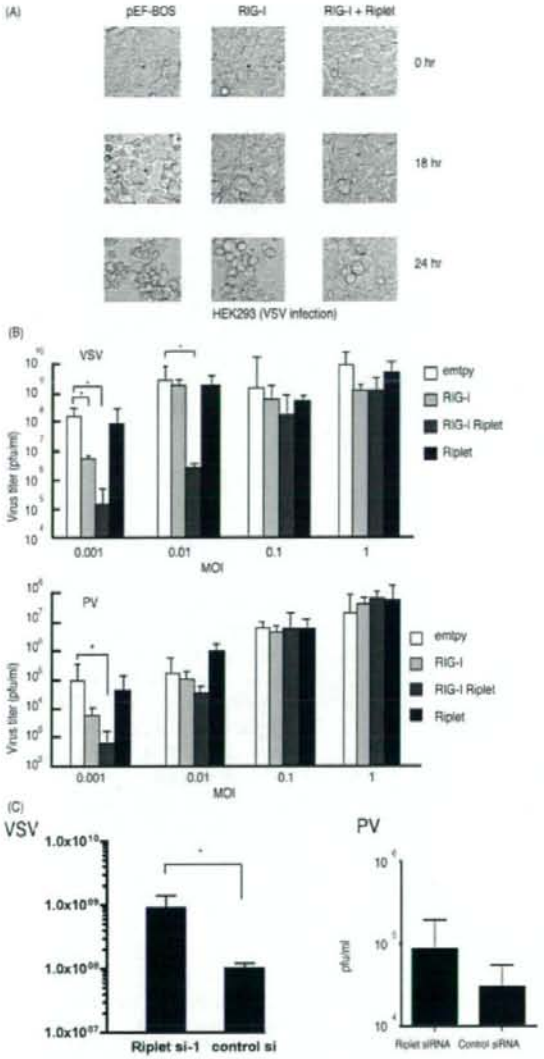

FIGURE 4. **Suppression of RNA viruses by Riplet.** *A*, HEK293 cells were transfected with RIG-I (0.1 μg) and/or Riplet (0.1 μg) expressing vectors. The total amount of transfected DNA (0.5 μg/well) in each well was kept constant by adding empty vector (pEF-BOS). 24 h after transfection, the cells were infected with VSV at m.o.i. = 0.1, and after 0, 18, or 24 h, CPE was observed by microscope. *B*, RIG-I (0.1 μg) and/or Riplet (0.1 μg) expressing plasmids were transfected to HEK293 cells in 24-well plates and incubated for 24 h. The total amount of transfected DNA (0.5 μg/well) in each well was kept constant by adding empty vector (pEF-BOS). The cells were infected with VSV (*upper panel*) or poliovirus (*PV*) (*lower panel*) at the indicated m.o.i. The viral titers in the culture media were measured 24 h after infection by plaque assay. *Error bars* represent standard deviation ($n = 3$). *, $p < 0.05$. *C*, control or Riplet knockdown HEK293 cells were infected with VSV (*left panel*) or poliovirus (*right panel*) at m.o.i. = 0.1. The viral titers in the culture media were measured 26 h after infection by plaque assays. Knockdown of Riplet induced higher VSV titers compared with control ($p < 0.05$), but the increase observed in poliovirus-infected Riplet knockdown cells was not significant ($p > 0.05$).

Riplet and Riplet-DN Bind the Helicase and RD Regions of RIG-I—Yeast two-hybrid analysis showed that a C-terminal region of Riplet bound to the C-terminal region of RIG-I. This cytoplasmic interaction between Riplet and RIG-I was confirmed by confocal microscopy in HeLa cells (supplemental Fig. S2). To further confirm the physical binding of Riplet to RIG-I in human cells, we carried out immunoprecipitation analyses. Full-length Riplet was co-immunoprecipitated with RIG-I (Fig. 5*B*), indicating that Riplet binds directly to RIG-I in human cells.

To determine the region responsible for the RIG-I-Riplet interaction, we constructed a RIG-I and Riplet deletion series as shown in Fig. 5*A*. Riplet-DN also bound to RIG-I (Fig. 5, *B* and *C*), indicating that the RING finger domain is dispensable for the RIG-I-Riplet interaction. This is consistent with the notion that the RING finger domain in ubiquitin ligase proteins is required for their interactions with ubiquitin-conjugating enzymes (29). Unlike TRIM25, Riplet and Riplet-DN failed to co-precipitate the two CARD domains of RIG-I (dRIG-I) (Fig. 5*D*). However, co-precipitation of the RIG-IC or RIG-RD fragments was observed (Fig. 5, *E* and *F*). RD-deleted RIG-I (RIG-I dRD) weakly associated with Riplet (Fig. 5*G*). Taken together, Riplet preferentially binds the RD and also weakly associates with the helicase region of RIG-I with its C terminus. Reporter gene analyses show that Riplet-DN only weakly suppresses RIG-I signaling and barely suppresses dRIG-I, which contains neither helicase nor RD region. Therefore, the physical interaction is correlated with the results of reporter activity.

Riplet Promotes Ubiquitination of RIG-I—Because Riplet shares 60% sequence similarity with TRIM25, we hypothesized that Riplet ubiquitinates RIG-I and that this modification leads to activation of RIG-I signaling. To test this hypothesis, we examined RIG-I ubiquitination. As expected, ubiquitination of RIG-I was increased by co-expression of Riplet under two different conditions (Fig. 6, *A* and *B*). The quantity of RIG-I ubiquitination was significantly high in the presence of Riplet (Fig. 6*C*). RIG-I ubiquitination was suppressed if Riplet was replaced with Riplet-DN (Fig. 6*D* and supplemental Fig. S4*C*). However, unlike TRIM25, Riplet binds to the C-terminal region of RIG-I. Therefore, we examined whether Riplet ubiquitinates the C-terminal region. We found that ubiquitination of RIG-IC was enhanced by Riplet expression (Fig. 6*E*). Both RIG-I dRD and RIG-I RD were also ubiquitinated by expression of Riplet (Fig. 6*F*; supplemental Fig. S4*A* and S5), suggesting that Riplet promotes ubiquitination of the helicase and RD domains of RIG-I in a manner distinct from TRIM25.

Ubiquitin is polymerized through its lysine residue. Lys-63-linked polyubiquitination is frequently observed in signal transduction pathways (30). In contrast, Lys-48-linked polyubiquitination usually leads to the degradation of protein through the proteasome. Indeed, TRIM25-mediated Lys-63-linked polyubiquitination activates the CARD-like region of RIG-I, and RNF125-mediated Lys-48-linked polyubiquitination leads to the degradation of RIG-I (23, 25). We used K48R or K63R mutated ubiquitin and found that K48R was incorporated normally into RIG-IC, whereas polyubiquitination was decreased by K63R (supplemental Fig. S4*B*). K63R mutation abolished RIG-I RD polyubiquitination by Riplet (Fig. 6*F*). These data

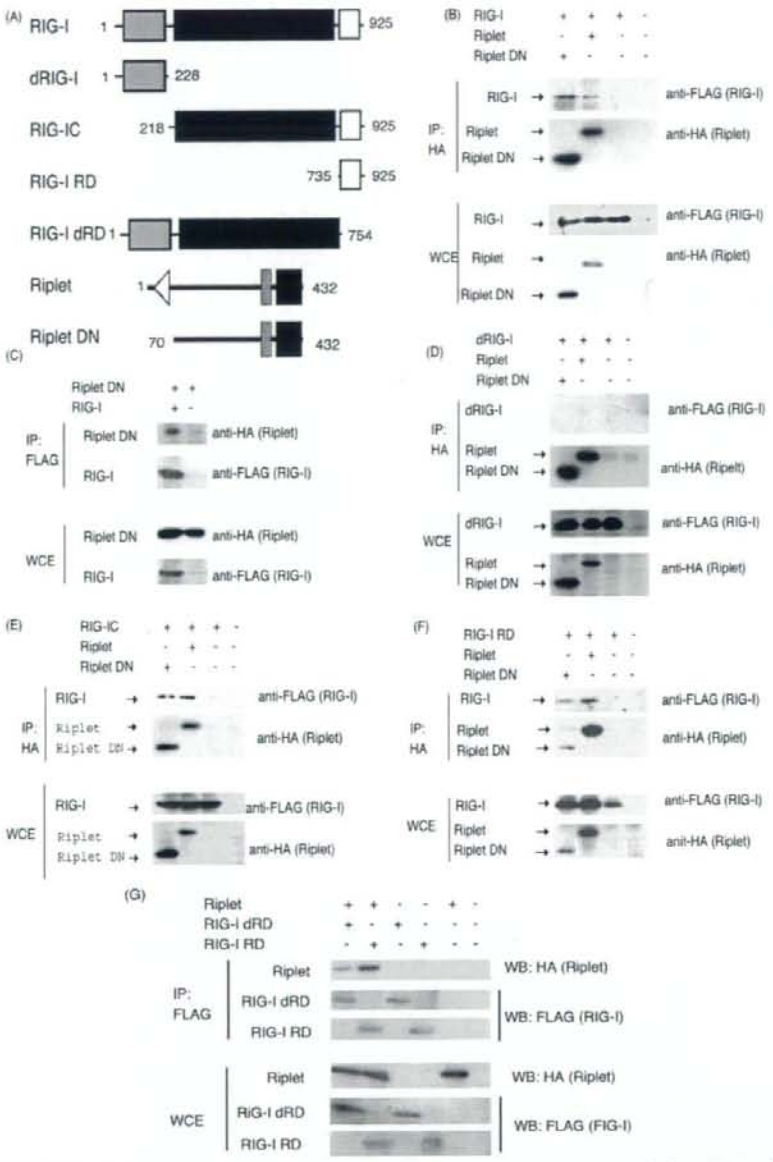

FIGURE 5. **Physical interaction of Riplet with RIG-I.** *A*, schematic representation of RIG-I or Riplet fragments used for immunoprecipitation analyses. *B*, HA-tagged Riplet (0.4 μg) or Riplet-DN (0.4 μg) were transfected into HEK293FT cells in a 6-well plate with FLAG-tagged RIG-I (0.4 μg). HA-tagged Riplet or Riplet-DN were immunoprecipitated (*IP*) with anti-HA antibodies, and samples were analyzed by Western blotting (*WB*) using an anti-FLAG or anti-HA antibody. The total amount of transfected DNA (2 μg/well) was kept constant by adding empty vector (pEF-BOS). *C*, HA-tagged Riplet-DN (0.4 μg) and FLAG-tagged RIG-I (0.4 μg) were transfected into HEK293FT cells in a 6-well plate. RIG-I was immunoprecipitated with anti-FLAG antibody, and samples were analyzed by Western blotting using an anti-FLAG or -HA antibody. The total amount of transfected DNA (2 μg/well) was kept constant by adding empty vector (pEF-BOS). *D–F*, interaction of HA-tagged Riplet or Riplet-DN with FLAG-tagged dRIG-I (*D*), RIG-IC (*E*), or RIG-I RD (*F*) was examined using immunoprecipitation assays. The proteins were expressed in HEK293FT cells, and HA-tagged Riplet was immunoprecipitated with anti-HA antibody, and samples were analyzed by Western blotting using an anti-FLAG or -HA antibody. *G*, FLAG-tagged RIG-I RD (0.4 μg) or RIG-I dRD (0.4 μg) was transfected with HA-tagged Riplet (0.4 μg) into HEK293 FT cells in a 6-well plate, and 24 h after transfection, immunoprecipitation was performed with anti-FLAG antibody and analyzed by Western blotting. The total amount of transfected DNA (2 μg/well) was kept constant by adding empty vector (pEF-BOS). *WCE*, whole cell extract.

indicates that Riplet mediates Lys-63-linked polyubiquitination of the RIG-I C-terminal helicase and RD region. Because Riplet-DN reduced the RIG-I-mediated signaling, we examined whether Riplet-DN reduced the RIG-I ubiquitination. As expected, Riplet-DN reduced RIG-I ubiquitination (Fig. 6*D* and supplemental Fig. S4*C*). These ubiquitination assay data are consistent with the notion that Riplet-mediated Lys-63-linked polyubiquitination of RIG-I is required for full activation of RIG-I signaling.

We tried to determine the ubiquitination sites of RIG-I using Lys-to-Ala (KA)-converting mutants. RIG-I has 25 Lys residues in its C-terminal region. These Lys residues of RIG-I were in turn mutated to Ala, and the degree of ubiquitination and IFN-β-inducing activity were determined with each mutant. RIG-I-mediated IFN-β promoter activation was normally augmented by co-expression of Riplet and 3KA RIG-I. Co-expression of Riplet and 5KA, however, and the ubiquitination level of RIG-I and IFN-β-inducing activity were simultaneously decreased (Fig. 7, *A* and *C*). Riplet-dependent augmentation of IFN-β promoter activation was largely suppressed when RIG-I was replaced with 5KA RIG-I (Fig. 7*B*). Therefore, Lys-849 and Lys-851 of RIG-I were crucial for RIG-I ubiquitination by Riplet. The results confirmed the importance of ubiquitination of specific Lys residues in the C-terminal region of RIG-I and for RIG-I-mediated IFN-β induction.

DISCUSSION

RIG-I plays a central role in the recognition of cytoplasmic viral RNA and is regulated by modification by small modifier ubiquitin or ubiquitin-like protein, ISG15. TRIM25 mediates Lys-63-linked polyubiquitination, which is essential for RIG-I activation (23), and RNF125 mediates Lys-48-linked polyubiquitination (25). RIG-I also harbors ISG15 modification, although the role of ISG15 modification *in vivo* remains to be deter-

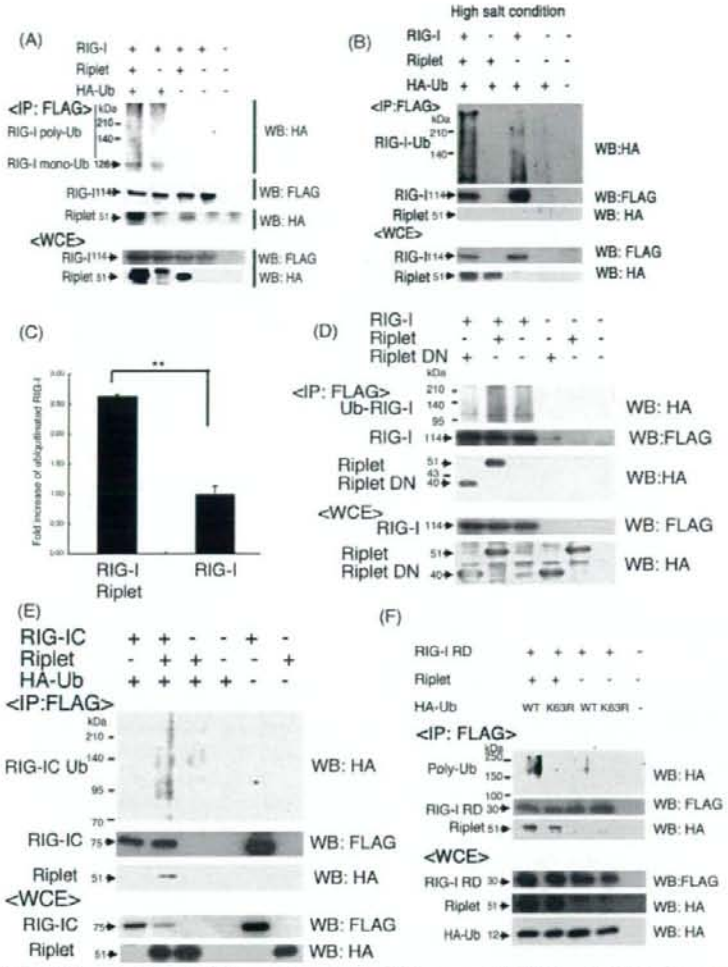

FIGURE 6. **Ubiquitination of RIG-I by Riplet.** *A* and *B*, FLAG-tagged RIG-I (0.4 μg), Riplet (0.4 μg), and HA-tagged ubiquitin (0.4 μg) expressing vectors were transfected into HEK293FT cells in 6-well plates. The total amount of transfected DNA (2 μg/well) was kept constant by adding empty vector (pEF-BOS). FLAG-tagged RIG-I was immunoprecipitated (*IP*) using an anti-FLAG antibody, and washed with the buffer containing 150 mM NaCl (*A*) or 1 M NaCl (*B*). The immunoprecipitates were separated with 8% acrylamide gel and analyzed by Western blotting (*WB*) using antibodies against HA tag (ubiquitin) or FLAG (RIG-I). Riplet was co-immunoprecipitated with FLAG-tagged RIG-I in *A* but could not co-immunoprecipitate in *B* because of high salt condition. Expression of Riplet enhanced the ubiquitination of RIG-I. Different gel conditions were employed in *A* and *B*. *C*, ubiquitinated RIG-I was quantitated with NIH image software. **, $p < 0.01$. *D*, FLAG-tagged RIG-I (0.4 μg) was transfected into HEK293 FT cells in a 6-well plate with HA-tagged Riplet (0.4 μg) or Riplet-DN (0.4 μg) and HA-tagged ubiquitin, and immunoprecipitation was carried out with anti-FLAG antibody. The total amount of transfected DNA (2 μg/well) was kept constant by adding empty vector (pEF-BOS). The samples were analyzed with 10% acrylamide gel to clearly separate Riplet from Riplet-DN and stained by Western blotting. *E*, ubiquitination of RIG-IC was also promoted by Riplet expression. HEK293FT cells were transfected with the plasmids encoding RIG-IC (0.4 μg), Riplet (0.4 μg), and/or HA-tagged ubiquitin (0.4 μg) in a 6-well plate, and 24 h after transfection, cell lysates were prepared. The total amount of transfected DNA (2 μg/well) was kept constant by adding empty vector (pEF-BOS). FLAG-tagged RIG-ICs were immunoprecipitated with anti-FLAG antibodies, and the proteins were analyzed by Western blotting. *F*, Ub-K63R are HA-tagged ubiquitin in which the lysine 3 residues were substituted with arginine. The HA-tagged Ub-K63 expressing vectors (1.2 μg), FLAG-tagged RIG-IC (0.4 μg), and/or Riplet (0.4 μg) were transfected into HEK293FT cells in 6-well plates and analyzed as shown in *A–D*. The total amount of transfected DNA (2 μg/well) was kept constant by adding empty vector (pEF-BOS). Ub-K63R was not incorporated into polyubiquitin chain of RIG-I RD. *WCE*, whole cell extract.

mined (21, 22, 31). Although Riplet and TRIM25 share 60% sequence similarity, the ubiquitination of RIG-I by Riplet is distinct from that by TRIM25; Riplet ubiquitinates the C-terminal region of RIG-I, whereas TRIM25 ubiquitinates its CARD-like region. These findings are also supported by the fact that neither Riplet nor Riplet-DN promoted or inhibited the activation of the IFN-β promoter by expression of the RIG-I CARD-like region (data not shown). It has been reported that ubiquitination of the CARD-like region of RIG-I by TRIM25 is critical for RIG-I-IPS-1 signaling (23). However, how this CARD ubiquitination is essential for activation of IPS-1 by RIG-I remains undetermined. Here we emphasize the importance of RIG-I C-terminal ubiquitination for IFN-β induction and the antiviral response. Because the C-terminal RD region inhibits the IFN inducing activity of the CARD-like region of RIG-I, it is reasonable that RIG-I C-terminal ubiquitination by Riplet inhibits the conversion from the active to inactive form of RIG-I protein after binding to viral RNA. This initial stabilization of RIG-I via ubiquitination by Riplet would provide a sufficient structure for RIG-I to maintain the accessibility to TRIM25 and facilitate TRIM25-mediated ubiquitination of the CARD-like region of RIG-I, which may lead to potential activation of IPS-1.

RIG-I is an IFN-inducible RNA helicase that is expressed at extremely low levels in resting cells (6). Initial penetration of viruses allows generation of 5′-triphosphate RNA and/or double strand RNA followed by induction of IFN-β production. This early response to viral infections triggers up-regulation of RIG-I/MDA5 and TLR3, leading to robust IFN-β production (3, 32, 33). We favor the interpretation of our present findings that during the early stages of viral infection with trace amounts of RIG-I and viral RNAs, Riplet helps host cells rearrange RIG-I conformation to activate IPS-1. This issue will need further proof because it is difficult to

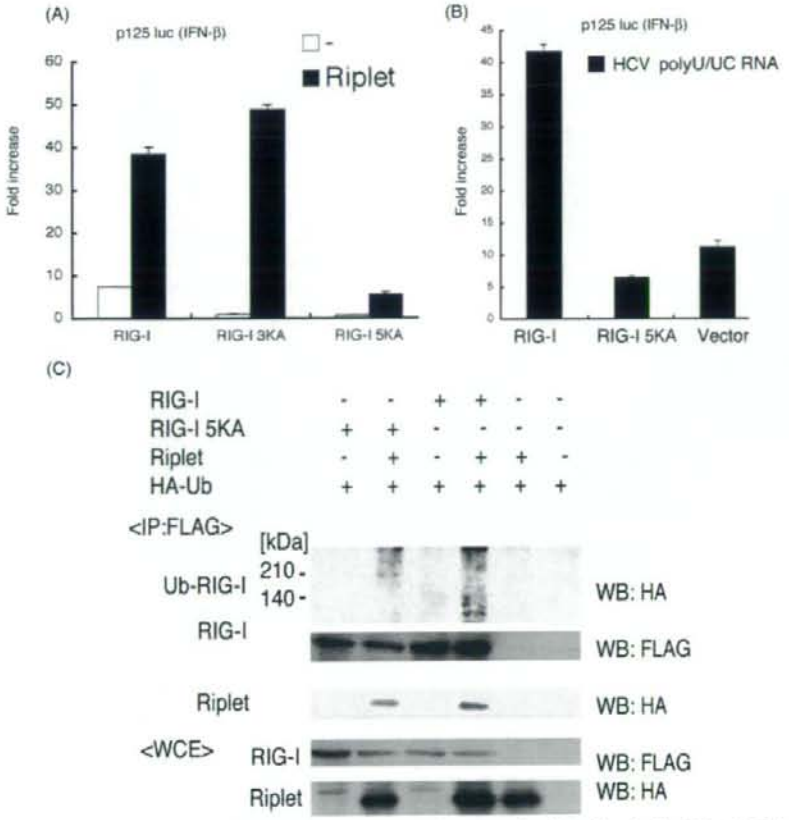

FIGURE 7. **The C-terminal two lysine residues of RIG-I are important for ubiquitination by Riplet.** *A*, RIG-I C-terminal lysine residues were substituted with alanine. RIG-I 3KA mutant protein harbors the triple mutations, K888A, K907A, and K909A. The five lysine residues, Lys-849, Lys-851, Lys-888, Lys-907, and Lys-909, were replaced with alanine in RIG-I 5KA mutant. The plasmid carrying wild-type (100 ng/well), RIG-I 3KA (100 ng/well), RIG-I 5KA (100 ng), or Riplet (100 ng) were transfected into HEK293 cells in a 24-well plate together with p125 luc reporter plasmid (100 ng/well). The amount of transfected DNA was kept constant by adding empty vector. After 24 h, the luciferase activities were measured. *B*, wild-type RIG-I (100 ng), RIG-I 5KA mutant (100 ng), or empty vector (100 ng) was transfected into HEK293 cells in a 24-well plate together with p125 luc reporter plasmids and HCV 3′-untranslated region poly(U/UC) RNA (25 ng), which is synthesized in *in vitro* transcription by T7 RNA polymerase. The amount of transfected DNA was kept constant by adding empty vector. 24 h after transfection, luciferase activities were measured. RIG-I 5KA mutant hardly responded to poly(U/UC) RNA. *C*, to observe the ubiquitinated RIG-I more clearly, we used 800 ng/well of Riplet and HA-Ub expression vector for the following transfection. HEK293FT cells in a 6-well plate were transfected with the plasmids encoding RIG-I (400 ng/well), RIG-I 5KA (400 ng/well), Riplet (800 ng/well), and/or HA-Ub (800 ng/well). The total amount of DNA was kept constant by adding the empty vector. 24 h after the transfection, the cell lysates were prepared, and the immunoprecipitation was carried out using anti-FLAG antibodies. The immunoprecipitates were analyzed by Western blotting with anti-HA or FLAG antibodies.

visualize RNRs and viral RNAs in the early infection stage and to understand the mechanisms that allow viruses to uncoat into naked viral RNA and to replicate.

We have provided several lines of evidence indicating that Riplet complements RIG-I-mediated IFN-β induction upon viral infection by both Riplet siRNA and overexpression analyses. The C-terminal lysines (849 and 851) of RIG-I are critical for Riplet-mediated RIG-I ubiquitination. However, our data indicate that Riplet alone was unable to induce IFN-β production and essentially required RIG-I to confer IFN-β induction. Furthermore, Riplet is not ubiquitously distributed over the organs tested. Ubiquitination of RIG-I induced by poly(I-C) or viruses was accelerated in cells pre-transfected with Riplet. Hence, Riplet works case-sensitive to up-regulate RIG-I antiviral activity predominantly in some organs. The physiological meaning of this response will be clarified by knock-out study.

Unexpectedly, the siRNA experiments were not robust with regard to VSV replication. Possible explanations for this are as follows: 1) the degree of gene silencing is not so profound that the proteins remain in the cells; 2) there are a number of virus-mediated IFN-inducing pathways capable of compensating each other, so that disruption of one factor does not cause a profound effect on VSV replication. Furthermore, in VSV-infected Riplet-knockdown cells, IFN-β levels were reduced even at m.o.i. = 1 (Fig. 3*D*), and accordingly, virus susceptibility was increased at m.o.i. = 0.1 (Fig. 4*C*), whereas in Riplet-overexpressing cells, antiviral activity was observed only at low m.o.i. (Fig. 4*B*). We used different transfection reagents and cell conditions in the knockdown and overexpression experiments to obtain high transfection efficiency in each. These conditional differences in knockdown and overexpression analyses might cause part of the discrepancy between the two results on Riplet antiviral activity. Another possibility to explain the apparent inconsistencies between overexpression and knockdown analyses is that high amounts of Riplet efficiently activate the RIG-I signaling, but low amounts are insufficient for RIG-I activation in high m.o.i.-infecting human cells. High amounts of Riplet with overexpressed RIG-I would confer the ability on cells to respond to very low amounts of VSV as observed in the low m.o.i. experiments. Again, *riplet* knock-out mice would reveal whether it is absolutely required for potential RIG-I activation.

How viral RNAs select RIG-I rather than dicers or the translation machinery is also unknown. During natural infection it is likely that the number of the initial invading virions would be at most several copies/cell. Uncoated viral RNA may assemble a complex consisting of viral and host molecules required for replication. We assume that cells are equipped with various

molecular arms to sensitively detect viral RNA. The molecular complexes sensing viral RNA may not be so simple that we will be able to identify more molecules than Riplet as enhancers for integral RNA recognition. In either case, yeast screening will be a good strategy to pick up such proteins in other RNA recognition systems. A molecular switch selecting IFN induction by virus RNA will then be clarified.

We show that the ubiquitination sites targeted by Riplet are the helicase and RD domains of RIG-I but not its CARD-like domains in contrast to TRIM25. Riplet may be a complement factor of the reported TRIM25 function for RIG-I activation (23). A previous report (25) failed to polyubiquitinate the RIG-I protein by TRIM25 alone. If Riplet were added to TRIM25 for RIG-I ubiquitination in the previous study, Riplet would have enabled TRIM25 to polyubiquitinate the RIG-I CARD-like region. Further studies using TRIM25 and Riplet will be required to clarify this point.

Based on our results, we propose that RIG-I-like receptors form a molecular complex that efficiently recognizes low copy numbers of viral RNA. Riplet is implicated in the RIG-I complex to enhance viral RNA response in some organs. In this context, MDA5-associated molecules might also exist in the cytoplasm to augment IFN output. Although MDA5 possesses the RD domain, it fails to recruit Riplet (data not shown) or augment IFN-β-induction in conjunction with Riplet (Fig. 2*E*). Because RLR-associated molecules naturally reside in cells and facilitate inhibition of low dose viral infection until RLRs become expressed, they may be useful therapeutic targets for an early phase antiviral immunotherapy.

Acknowledgments—We thank Dr. M. Sasai in our laboratory for technical instructions for assay of RIG-I functions and Drs. K. Shimotohno (Keio University), T. Taniguchi (University of Tokyo), and T. Fujita (Kyoto University) for their critical discussions.

REFERENCES

1. Takeuchi, O., and Akira, S. (2008) *Curr. Opin. Immunol.* **20,** 17–22
2. Honda, K., Takaoka, A., and Taniguchi, T. (2006) *Immunity* **25,** 349–360
3. Kato, H., Takeuchi, O., Sato, S., Yoneyama, M., Yamamoto, M., Matsui, K., Uematsu, S., Jung, A., Kawai, T., Ishii, K. J., Yamaguchi, O., Otsu, K., Tsujimura, T., Koh, C. S., Reis e Sousa, C., Matsuura, Y., Fujita, T., and Akira, S. (2006) *Nature* **441,** 101–105
4. Venkataraman, T., Valdes, M., Elsby, R., Kakuta, S., Caceres, G., Saijo, S., Iwakura, Y., and Barber, G. N. (2007) *J. Immunol.* **178,** 6444–6455
5. Yoneyama, M., Kikuchi, M., Matsumoto, K., Imaizumi, T., Miyagishi, M., Taira, K., Foy, E., Loo, Y. M., Gale, M., Jr., Akira, S., Yonehara, S., Kato, A., and Fujita, T. (2005) *J. Immunol.* **175,** 2851–2858
6. Yoneyama, M., Kikuchi, M., Natsukawa, T., Shinobu, N., Imaizumi, T., Miyagishi, M., Taira, K., Akira, S., and Fujita, T. (2004) *Nat. Immunol.* **5,** 730–737
7. Hornung, V., Ellegast, J., Kim, S., Brzozka, K., Jung, A., Kato, H., Poeck, H., Akira, S., Conzelmann, K. K., Schlee, M., Endres, S., and Hartmann, G. (2006) *Science* **314,** 994–997
8. Pichlmair, A., Schulz, O., Tan, C. P., Naslund, T. I., Liljestrom, P., Weber, F., and Reis e Sousa, C. (2006) *Science* **314,** 997–1001
9. Saito, T., Hirai, R., Loo, Y. M., Owen, D., Johnson, C. L., Sinha, S. C., Akira, S., Fujita, T., and Gale, M., Jr. (2007) *Proc. Natl. Acad. Sci. U. S. A.* **104,** 582–587
10. Kawai, T., Takahashi, K., Sato, S., Coban, C., Kumar, H., Kato, H., Ishii, K. J., Takeuchi, O., and Akira, S. (2005) *Nat. Immunol.* **6,** 981–988
11. Meylan, E., Curran, J., Hofmann, K., Moradpour, D., Binder, M., Bartenschlager, R., and Tschopp, J. (2005) *Nature* **437,** 1167–1172
12. Seth, R. B., Sun, L., Ea, C. K., and Chen, Z. J. (2005) *Cell* **122,** 669–682
13. Xu, L. G., Wang, Y. Y., Han, K. J., Li, L. Y., Zhai, Z., and Shu, H. B. (2005) *Mol. Cell* **19,** 727–740
14. Rothenfusser, S., Goutagny, N., DiPerna, G., Gong, M., Monks, B. G., Schoenemeyer, A., Yamamoto, M., Akira, S., and Fitzgerald, K. A. (2005) *J. Immunol.* **175,** 5260–5268
15. Loo, Y. M., Fornek, J., Crochet, N., Bajwa, G., Perwitasari, O., Martinez-Sobrido, L., Akira, S., Gill, M. A., Garcia-Sastre, A., Katze, M. G., and Gale, M., Jr. (2008) *J. Virol.* **82,** 335–345
16. Komuro, A., and Horvath, C. M. (2006) *J. Virol.* **80,** 12332–12342
17. McWhirter, S. M., Tenoever, B. R., and Maniatis, T. (2005) *Cell* **122,** 645–647
18. Saha, S. K., Pietras, E. M., He, J. Q., Kang, J. R., Liu, S. Y., Oganesyan, G., Shahangian, A., Zarnegar, B., Shiba, T. L., Wang, Y., and Cheng, G. (2006) *EMBO J.* **25,** 3257–3263
19. Kayagaki, N., Phung, Q., Chan, S., Chaudhari, R., Quan, C., O'Rourke, K. M., Eby, M., Pietras, E., Cheng, G., Bazan, J. F., Zhang, Z., Arnott, D., and Dixit, V. M. (2007) *Science* **318,** 1628–1632
20. Lin, R., Yang, L., Nakhaei, P., Sun, Q., Sharif-Askari, E., Julkunen, I., and Hiscott, J. (2006) *J. Biol. Chem.* **281,** 2095–2103
21. Zhao, C., Denison, C., Huibregtse, J. M., Gygi, S., and Krug, R. M. (2005) *Proc. Natl. Acad. Sci. U. S. A.* **102,** 10200–10205
22. Arimoto, K., Konishi, H., and Shimotohno, K. (2008) *Mol. Immunol.* **45,** 1078–1084
23. Gack, M. U., Shin, Y. C., Joo, C. H., Urano, T., Liang, C., Sun, L., Takeuchi, O., Akira, S., Chen, Z., Inoue, S., and Jung, J. U. (2007) *Nature* **446,** 916–920
24. Urano, T., Saito, T., Tsukui, T., Fujita, M., Hosoi, T., Muramatsu, M., Ouchi, Y., and Inoue, S. (2002) *Nature* **417,** 871–875
25. Arimoto, K., Takahashi, H., Hishiki, T., Konishi, H., Fujita, T., and Shimotohno, K. (2007) *Proc. Natl. Acad. Sci. U. S. A.* **104,** 7500–7505
26. Sasai, M., Shingai, M., Funami, K., Yoneyama, M., Fujita, T., Matsumoto, M., and Seya, T. (2006) *J. Immunol.* **177,** 8676–8683
27. Douglas, J., Cilliers, D., Coleman, K., Tatton-Brown, K., Barker, K., Bernhard, B., Burn, J., Huson, S., Josifova, D., Lacombe, D., Malik, M., Mansour, S., Reid, E., Cormier-Daire, V., Cole, T., and Rahman, N. (2007) *Nat. Genet.* **39,** 963–965
28. Barral, P. M., Morrison, J. M., Drahos, J., Gupta, P., Sarkar, D., Fisher, P. B., and Racaniello, V. R. (2007) *J. Virol.* **81,** 3677–3684
29. Seol, J. H., Feldman, R. M., Zachariae, W., Shevchenko, A., Correll, C. C., Lyapina, S., Chi, Y., Galova, M., Claypool, J., Sandmeyer, S., Nasmyth, K., Deshaies, R. J., Shevchenko, A., and Deshaies, R. J. (1999) *Genes Dev.* **13,** 1614–1626
30. Pickart, C. M. (2004) *Cell* **116,** 181–190
31. Kim, M. J., Hwang, S. Y., Imaizumi, T., and Yoo, J. Y. (2008) *J. Virol.* **82,** 1474–1483
32. Alexopoulou, L., Holt, A. C., Medzhitov, R., and Flavell, R. A. (2001) *Nature* **413,** 732–738
33. Tanabe, M., Kurita-Taniguchi, M., Takeuchi, K., Takeda, M., Ayata, M., Ogura, H., Matsumoto, M., and Seya, T. (2003) *Biochem. Biophys. Res. Commun.* **311,** 39–48
34. Yoneyama, M., Suhara, W., Fukuhara, Y., Fukuda, M., Nishida, E., and Fujita, T. (1998) *EMBO J.* **17,** 1087–1095

International Immunology, Vol. 20, No. 9, pp. 1169–1180
doi:10.1093/intimm/dxn074

Soluble G protein of respiratory syncytial virus inhibits Toll-like receptor 3/4-mediated IFN-beta induction

Masashi Shingai[1,4], Masahiro Azuma[1], Takashi Ebihara[1], Miwa Sasai[1,5], Kenji Funami[1,6], Minoru Ayata[2], Hisashi Ogura[2], Hiroyuki Tsutsumi[3], Misako Matsumoto[1] and **Tsukasa Seya[1]**

[1]Department of Microbiology and Immunology, Hokkaido University Graduate School of Medicine, Kita-15, Nishi-7, Kita-ku, Sapporo 060-8638, Japan
[2]Department of Virology, Osaka City University, Asahimachi 1-4-3, Abeno-ku, Osaka 545-8585, Japan
[3]Department of Pediatrics, Sapporo Medical University, School of Medicine, Minami-1, Nishi-16, Chuoh-ku, Sapporo 060-8543, Japan

[4]Present address: Laboratory of Molecular Microbiology, National Institute of Allergy and Infectious Diseases, National Institutes of Health, Bethesda, MD 20892, USA
[5]Present address: Section of Immunobiology, Yale University School of Medicine, 300 Cedar Street, TAC S640, New Haven, CT 06520, USA
[6]Present address: Medical Research Center, Keio University, Shinanomachi 35, Shinjuku-ku, Tokyo 160-8582, Japan

Keywords: dendritic cells, respiratory syncytial virus, TICAM-1 (TRIF), Toll-like receptor, type I IFNs

Abstract

Monocyte-derived dendritic cells (mDCs) recognize viral RNA extrinsically by Toll-like receptor (TLR) 3 on the membrane and intrinsically retinoic acid-inducible gene I (RIG-I)/melanoma differentiation-associated gene 5 (MDA5) in the cytoplasm to induce type I IFNs and mDC maturation. When mDCs were treated with live or UV-irradiated respiratory syncytial virus (RSV), early (~4 h) induction of IFN-β usually occurs in other virus infections was barely observed. Live RSV subsequently replicated to activate the cytoplasmic IFN-inducing pathway leading to robust type I IFN induction. We found that RSV initial attachment to cells blocked polyI:C-mediated IFN-β induction, and this early IFN-β-modulating event was abrogated by antibodies against envelope proteins of RSV, demonstrating the presence of a IFN-regulatory mode by early RSV attachment to host cells. By IFN-stimulated response element (ISRE) reporter analysis in HEK293 cells, polyI:C- or LPS-mediated ISRE activation was dose dependently inhibited by live and inactive RSV to a similar extent. Of the RSV envelope proteins, simultaneously expressed or exogenously added RSV G or soluble G (sG) proteins inhibited TLR3/4-mediated ISRE activation in HEK293 cells. sG proteins expressed in cells did not affect the RIG-I/MDA5 pathway but inhibited the TLR adaptor TRIF/TICAM-1 pathway for ISRE activation. Finally, extrinsically added sG protein suppressed the production of IFN-β in mDCs. Although the molecular mechanism of this extrinsic functional mode of the RSV G glycoprotein (G protein) remains undetermined, G proteins may neutralize the fusion glycoprotein function that promotes IFN-mediated mDC modulation via TLR4 and may cause insufficient raising cell-mediated immunity against RSV.

Introduction

Respiratory syncytial virus (RSV) is a member of the Paramyxoviridae family consisting of a negative-strand RNA genome in a nucleocapsid. RSV preferentially infects airway epithelial cells, causing bronchiolitis and respiratory infections (1) and can exacerbate asthma and chronic obstructive pulmonary diseases (1). However, an effective vaccine for RSV is not yet available. Recurrent RSV infections are often observed in humans, and this is due to the failure of the hosts to raise long-lasting immunity against RSV (1). Recent reports suggested that cell-mediated immunity, including CTLs, NK and B cells, develops followed by maturation of monocyte-derived dendritic cells (mDCs) (2). These

Correspondence to: T. Seya; E-mail: seya-tu@pop.med.hokudai.ac.jp

Transmitting editor: T. Takai

Received 20 September 2007, *accepted* 9 June 2008

Advance Access publication 8 July 2008

lymphocytes produce IFN-γ which orchestrates the acquired immune response to eradicate viral infection (3). Toll-like receptors (TLRs), retinoic acid-inducible gene I (RIG-I)-like receptors and NOD-like receptors are expressed in dendritic cells (DCs) and play a major role in driving the lymphocyte-mediated immune responses (4). Possible involvement of TLR3 and its response in RSV infectious signs has been reported (5–7), although how RSV induces host immune modulation via the TLR3 remains largely unclear.

Type I IFNs serve as antiviral factors. Several reports have suggested the involvement of TLR3 (5, 7) and RIG-I (6) in RSV-mediated IFN-α/β induction and cellular responses. RIG-I preferentially recognizes 5′-triphosphate RNA (8, 9) in addition to double-stranded (ds)RNA, whereas TLR3 captures only dsRNA. Their signaling pathways partially overlap in that they converge upon the IFN-regulatory factor (IRF)-3-activating kinase complex for activation of the IFN-β promoter (10). Bronchial epithelial cells and mDCs preserve these receptors and downstream signaling pathways. mDC TLR3 particularly plays a crucial role in driving mDCs to direct CTL- and NK-inducing maturation as well as RSV infection-mediated type I IFN production (11, 12).

For induction of type I IFNs and NK/CTL activation, the cytoplasmic Toll–IL-1R (TIR) homology domain of TLR3 recruits the adaptor molecule TICAM-1 (TRIF) (13, 14), while LPS allows TLR4 to recruit the adaptor molecules TICAM-2 (TRAM) and TICAM-1 (15, 16). Thus, TICAM-1 is the common adaptor in the pathways of TLR3 and TLR4. Both pathways activate IRF-3 and IRF-7 through a MyD88-independent pathway, resulting in IFN-β production. Extrinsic supplement of viral dsRNA can activate the TICAM-1 pathway (17). On the other hand, RIG-I and melanoma differentiation-associated gene 5 (MDA5) reside in the cytoplasm and interact with a mitochondrial protein, IFN-β promoter stimulator 1 (IPS-1)/mitochondria antiviral signaling (MAVS)/VISA/Cardif, to activate IRF-3 and IRF-7 (18–21). Only intrinsically produced viral RNA is a ligand for the cytoplasmic IFN-inducing sensors. Studies on how these pathways evoke mDC-mediated cellular immunity are in progress with special interest (22). Although there is a MyD88-dependent pathway for IFN induction in plasmacytoid DCs (23–25), this pathway does not function in mDCs. Accordingly, we focus on the role of the TICAM-1 and IPS-1 pathways in RSV-mediated mDC functional modulation.

In the virus side, what RSV factors are associated with modulation of mDC maturation remain largely unknown. In cytoplasmic RSV proteins, the NS1 and NS2 proteins are shown to antagonize IFN response (26, 27). Nevertheless, type I IFN is induced in RSV-replicating cells although the amounts of IFN are relatively low. The envelope of RSV contains three transmembrane surface proteins, the fusion glycoprotein (F protein), G glycoprotein (G protein) and SH protein. F protein is responsible for fusion of the viral envelope with the plasma membrane of the host target cell (28). The F protein may induce activation of nuclear factor-κB (NF-κB) and the IFN-β promoter via TLR4 (29, 30). In addition, the F protein of RSV serves as an agonist of TLR4 and induces pro-inflammatory cytokines (29). On the other hand, the G protein, which mediates attachment of the virus particle to the target cell (31), and SH protein are not functionally well understood (32). Infected cells also produce a smaller secreted form of the G protein [soluble G (sG) protein] besides the transmembrane type G protein (33). The RSV G protein has been implicated in altered cytokine and chemokine expression by pulmonary leukocytes (34). Yet, there has been no report on the RSV surface proteins that affect cytoplasmic IFN-inducing events. Accordingly, no report has mentioned the possible association between the RSV G/SH proteins and the TLR pathways in RSV infection.

Here, we discovered a role of the RSV G protein in mDC IFN response. This protein inhibits the TLR3/4-mediated IFN-β promoter activation through RSV–host cell interaction. A possible target for the G protein attachment to cells is the TICAM-1 pathway, thereby TLR3/4-mediated type I IFN induction being prohibited. The RSV G protein may act as a buffer for evoking cell-mediated TLR3/4-derived immunity. Possible roles for the function of the G protein in the RSV infection are also discussed.

Methods

Cell culture, viruses and reagents

HEp-2, Vero and HEK293 cells were maintained in DMEM (Invitrogen, San Diego, CA, USA) supplemented with 10% heat-inactivated FCS (JRH Biosciences, Lenexa, KS, USA) and antibiotics. Human RSV field-isolate strain (RSV2177) in subgroup B was isolated and propagated with HEp-2 cells. The accession numbers of *NS1*, *NS2*, *N*, *G*, *F* and *SH* genes were AB245473–AB245478. The titer of RSV2177 was determined by 50% tissue culture infective dose with HEp-2 cells. Measles virus (MV) Edmonston strain was passaged and titrated in Vero cells. RSV and MV were inactivated by UV irradiation at 1.5 J cm^{-2}. Poly I:C was purchased from Amersham Pharmacia Biotech (Buckinghamshire, UK). Polymyxin B, LPS from *Escherichia coli* serotype 0111:B4, was from Sigma Chemical Co., St Louis, MO, USA. The mycoplasma lipopeptide macrophage-activating lipopeptide-2 (MALP-2) was prepared as described (35). MALP-2 and poly I:C were treated with polymyxin B (10 μg ml^{-1}) (an LPS inhibitor) for 1 h at 37°C before stimulation of cells (35). Usually, 50 or 10 μg ml^{-1} of poly I:C, 100 ng ml^{-1} of LPS and 100 nM of MALP-2 were utilized for TLR stimulation. Mouse IgG, mouse IgG2b and anti-Flag M2 mAb and anti-Flag polyclonal antibodies were obtained from Sigma; anti-CD80 and anti-HLA-DR mAbs were obtained from Immunotech (Marseille, France); anti-CD83 mAb was obtained from Cosmo Bio (Tokyo, Japan); anti-CD86 mAb was obtained from Ancell (Bayport, MN, USA); anti-CD40 mAb was from PharMingen (San Diego, CA, USA); FITC-conjugated goat anti-mouse and anti-rabbit IgG $F(ab')_2$ and HRP-conjugated goat anti-rabbit Igs were obtained from American Qualex Manufacturers (Bayport San Clemente, CA, USA) and FITC-labeled and non-labeled goat anti-RSV polyclonal antibody was from Chemicon.

Preparation of DCs (mDCs)

Human PBMCs were isolated from buffy coat of normal healthy donors by methylcellulose sedimentation followed by standard density-gradient centrifugation with Ficoll–Hypaque (Amersham Biosciences, Piscataway, NJ, USA) (35). For human immature DC preparation, CD14-positive monocytes

were prepared from huPBMC by using MACS system (Miltenyi Biotec, Gladbach, Germany) with anti-human CD14 mAb-conjugated microbeads and kept in RPMI-1640 (Invitrogen) containing 10% FCS, 500 IU ml^{-1} human granulocyte macrophage colony-stimulating factor, 100 IU ml^{-1} human IL-4 (Pepro Tech, London, UK) and antibiotics for 6 days. Morphological changes were examined by phase contrast microscopy (Olympus IX-70, Tokyo, Japan).

FACS cytometric analysis of cell-surface antigens

FACS methods were described previously (35). Briefly, cells were suspended in PBS containing 0.1% sodium azide and 1% BSA (FACS buffer) and incubated for 30 min at 4°C with relevant or control mAbs, followed by FITC-labeled anti-mouse IgG $F(ab')_2$. In some experiments, cells were directly stained with FITC-labeled anti-RSV polyclonal antibody. Cells were washed, and their fluorescence intensities were measured by FACS.

Determination of human tumor necrosis factor-α and IFN-β level

Quantitative PCR and ELISA were used for this purpose. Culture media were centrifuged to remove cell debris and the supernatants were stored at −80°C until the assay. The level of secreted human tumor necrosis factor-α (TNF-α) or IFN-β in the culture medium was determined with ELISA kits (Amersham Pharmacia and FUJIREBIO, Tokyo, Japan). The detection limits of human TNF-α and IFN-β were <5 pg ml^{-1} and <2.5 U ml^{-1}, respectively. Quantitative PCR and the primers for this assay were performed as described previously (36).

RSV sequences and plasmid construction

Total RNA from RSV2177-infected HEp-2 cells was extracted with RNeasy mini kit (Qiagen). After DNase treating, 1 μg of total RNA was incubated at 70°C for 5 min, kept on ice for 2 min and reverse transcription was performed with MMLV–reverse transcriptase (Promega, Madison, WI, USA) at 37°C for 90 min followed by PCR. Detection of RSV subgroup was performed by PCR with subgroup-specific primer sets (37) (RSV/SH A 5′-TCGAGTCAACACATAGCATTC-3′ and RSV/F1 5′-CAACTCCATTGTTATTTGCC-3′ for RSV subgroup A and RSV/SH B 5′-CATAGTATTCTACCATTATGC-3′ and RSV/F1 for RSV subgroup B). Direct sequences were detected from the amplified PCR fragments with conserved sequence primer sets among RSVs (RSV/Fm01 5′-GGCAAATAACAATGGAGYTGC-3′ and RSV/Fg01 5′-TTGTWRRAACATGATYAGGTG-3′ for F gene, RSV/Gm01 5′-GGCAAATGCAACCATGTCCAA-3′ and RSV/Gg01 5′-ACCCAATCACATGCTTAGTTATTC-3′ for G gene, RSV/SHm01 5′-ATGGGAAATACATCCAT-3′ and RSV/SHg01 5′-CACAGCATAATGGTAGA-3′ for SH gene and RSV/NPm01 5′-ATGGCTCTTAGCAAAG-3′ and RSV/NPg01 5′-TTAAAGCTCTACATCAT-3′ for NP gene). The nucleotide sequences of these PCR fragments were confirmed by direct sequencing. The consensus sequences obtained from the amplicons were inserted into a plasmid vector (pEFBos or $pCXN_2$), and the clones were modified by addition of Flag-tag, exchanging of signal sequence and/or truncation of the cytoplasmic and transmembrane regions.

Plasmid transfection and luciferase assay

A luciferase reporter plasmid, pISRE-Luc, was from Stratagene (Stratagene, La Jolla, CA, USA) and pELAM-Luc reporter plasmid was constructed as referred in Kurt-Jones *et al.* (29). pRL-TK vector was from Promega. A plasmid for human TLR3 and TICAM-1 expression was described previously (13). Plasmids for human TLR4, MD-2 and CD14 expression were kindly provided by K. Miyake (The University of Tokyo, Tokyo), TANK-binding kinase 1 (TBK1) expression by M. Nakanishi (The Nagoya City University, Nagoya) and IκB kinase-related kinase ε (IKKε) expression by T. Maniatis (Harvard Medical School, Boston, MA, USA). Plasmids for constitutive active forms of RIG-I and MDA5 (ΔRIG-I and MDA5N) expression were kindly provided by T. Fujita (The University of Kyoto, Kyoto). All transfection was carried out on HEK293 cells growing on 24-well plates. Usually, 100 ng of TLR3/pEFBos or TLR4/pEFBos, 100 ng of MD-2/pEFBos, 100 ng of CD14/pEFBos, 100 ng of luciferase reporter gene plasmid (firefly luciferase, experimental reporter) and 3 ng of pRL-TK vector (Renilla luciferase for internal control) were introduced into cells by LipofectAMINE 2000 (Invitrogen) according to the manufacture's procedure. At 24 h post-transfection, cells were stimulated with various stimulators for 6 h. Cells were then harvested with trypsin, washed with PBS and treated with 20 μl of Passive Lysis Buffer (Promega). After 6-h incubation, cells were lysed with lysis buffer and the assay was performed using dual-luciferase reporter assay system. Fold induction against the control medium is indicated.

Immunoprecipitation, SDS–PAGE and western blotting

Cells were washed in PBS (pH 7.4) and solubilized with 100 μl of 1% (v/v) Triton X-100 containing 137 mM NaCl, 2 mM EDTA and 1 mM phenylmethylsulfonylfluoride. After centrifugation (10 000 × *g* for 10 min), proteins in cell lysate or culture supernatant were immunoprecipitated with anti-Flag mAb. Immunoprecipitants were washed and eluted with Flag peptide. The eluted samples were heated or non-heated and were subjected to SDS–PAGE under reducing or non-reducing conditions. Proteins were transferred onto nylon membranes. The membranes were incubated with 10% skimmed milk containing 5% goat serum for 30 min at room temperature, followed by the addition of anti-Flag pAbs. One hour later, the membranes were washed extensively with PBS containing 0.5% Tween 20 and then incubated with 5 μg of HRP-conjugated goat anti-rabbit IgG antibody for 1 h at 37°C. Following second incubation, the membranes were washed with PBS–Tween 20 and proteins were detected with an ECL chemiluminescence kit (Amersham Biosciences).

Endoglycosidase digestion

Protein samples were made up to a final concentration of either 100 mM Tris–HCl (pH 8.6), 0.1% SDS and 1% NP-40 or 50 mM sodium citrate (pH 5.0) and 0.5% SDS and incubated at 37°C for 14 h with endoglycosidase F (Takara) or endoglycosidase H (Seikagaku Corporation, Tokyo, Japan), respectively, as previously reported (38). The samples were analyzed on SDS–PAGE under reducing and non-reducing conditions.

RSV treatment of human cells

Human cells (mDCs and HEK293 cells) were transfected with pGV-E2/huELAM (ELAM promoter-linked firefly luciferase) or pISRE-Luc [IFN-stimulated response element (ISRE) promoter-linked firefly luciferase] and phRL-TK (thymidin kinase with Renilla luciferase). The last one is the internal control. Twenty-four hours later, cells were washed and treated with live or UV-irradiated RSV [multiplicity of infection (MOI) = 0.5, otherwise indicated], LPS or medium. In some experiments, antibodies against RSV proteins (20 μg ml^{-1}) were added to the cells together with UV-irradiated RSV (MOI = 1.0). The cells were lysed with lysis buffer at the indicated time points and the assay was performed using dual-luciferase reporter assay system. Fold induction against the control medium is indicated at each time point.

Inhibitory effect of the sG protein on the ISRE promoter was tested as follows. The supernatant containing the secreted G protein, UV-irradiated RSV, UV-irradiated MV or medium were added to HEK293 cells, and then cells were transfected with TICAM-1/pEFBos (50 ng), IKKε/pcDNA3.1 (200 ng), TBK1/pcDNA3.1 (200 ng), MAVS/pEFBos (400 ng), ΔRIG-I/pEFBos (700 ng) or MDA5N/pEFBos or pEFBos (700 ng) and 100 ng of pISRE and 3 ng of pRL-TK. Six hours later, cells were harvested with trypsin, washed with PBS and treated with 20 μl of Passive Lysis Buffer. Luciferase activities were measured by Dual-Luciferase assay kit (Promega). The luciferase activity of firefly was normalized by that of Renilla and relative fold activation to the medium control was determined. All experiments were performed in triplicate.

Results

Immune responses induced in human DCs by RSV stimulation

DCs in the respiratory tract play important roles in the immune response against RSV infection. Human mDCs prepared from three healthy donors were incubated with RSV at MOI = 0.5. Viral proteins were detected on the mDC surface within 24 h and kept expressed over 48 h using anti-RSV polyclonal antibodies by FACS analysis (Fig. 1A). Thus, human mDCs are susceptible to RSV of this subgroup B isolate.

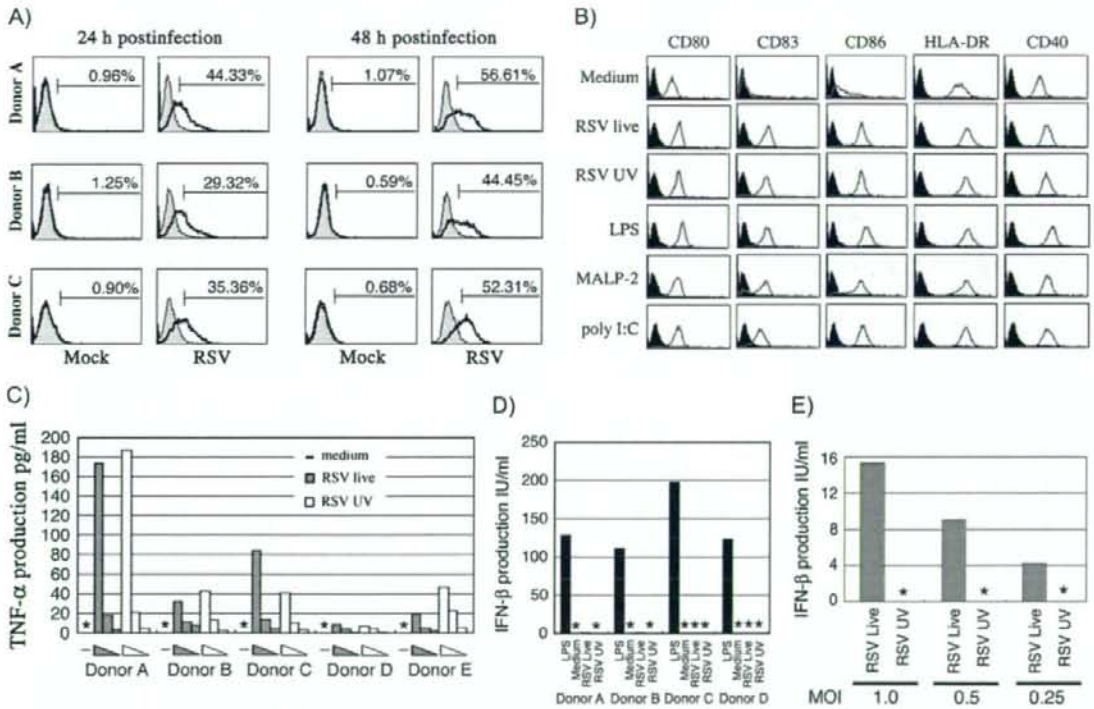

Fig. 1. Human DCs responding to RSV. (Panel A) Human immature mDCs are susceptible to RSV infection. Immature mDCs were incubated with Mock or RSV (MOI = 0.5). These mDCs were stained with FITC-labeled goat anti-RSV polyclonal antibodies or FITC-labeled control mouse Ig 24 or 48 h after RSV infection. %RSV-positive cells are indicated in the FACS histograms. (Panel B) mDC maturation is induced by RSV treatment. Immature mDCs were treated with indicated TLR ligands, medium only or RSV (live or UV irradiated, MOI = 0.5). Twenty-four hours later, mDCs were allowed to react with the indicated antibodies of $F(ab')_2$ against mDC maturation markers (open histograms). Isotype-matched IgG was used as controls (closed histograms). The experiments were performed three times and represented results are shown. (Panel C) Production of TNF-α by mDCs treated with live or UV-irradiated RSV. Human immature mDCs were prepared from five healthy donors and individually treated with RSV (live or UV irradiated) at MOI = 0.5, 0.25 and 0.1. The culture supernatants of the mDCs were harvested in 24 h and the levels of TNF-α determined by ELISA. Asterisk means 'not detected'. (Panels D and E) Production of IFN-β by mDCs in response to RSV. Immature mDCs were treated with RSV (live or UV irradiated) at MOI = 0.5 (otherwise indicated). LPS (100 ng ml^{-1}) or medium were used as controls. Twenty-four hours later, the supernatants were collected, and the levels of IFN-β were measured by ELISA. Asterisk, not detected.

To examine DC maturation by RSV, mDCs were stimulated with live or UV-irradiated RSV, LPS (TLR4 ligand), MALP-2 (TLR2 ligand) or polyI:C (TLR3 ligand) (Fig. 1B). Stimulation with either live or UV-irradiated RSV led to maturation of mDC as determined by cell-surface markers (CD80, CD83, CD86, HLA-DR and CD40) as was the case with the other TLR ligands. Since UV-irradiated RSV induced mDC maturation, RNA replication after viral entry is not a main cause for the RSV-mediated mDC maturation.

Next, we examined if mDCs produce TNF-α and IFN-β in response to RSV infection/stimulation. TNF-α is induced mainly through NF-κB activation and known to mature mDCs. mDCs from various individuals were incubated with the indicated doses of live or UV-irradiated RSV (Fig. 1C). LPS was used as a positive control for the TLR4 ligand. Twenty-four hours later, the supernatants were collected for ELISA. The levels of TNF-α were increased in the supernatant of mDCs in a RSV dose-dependent manner irrespective of RSV treatment, live or UV irradiation (Fig. 1C). Thus, viral attachment to cells rather than replication triggers TNF-α production. However, IFN-β was barely produced in mDCs treated with RSV (Fig. 1D). Although higher doses of live RSV minimally induce IFN-β (<20 IU ml^{-1}) in mDCs during 24 h (i.e. replication dependently, presumably via the cytoplasmic pathway), UV-irradiated RSV did not induce IFN-β by MOI = 1.0 (Fig. 1E) and even at MOI = 5 (data not shown). Although IFN-β induction appears to occur by stimulation of TLR4 with the F protein (30), this is not the case in challenge with UV-irradiated RSV. mDC maturation with TNF-α production but poor IFN-β production is a characteristic phenotype in RSV-affected human mDCs.

Quantitative PCR analysis was performed with mDCs for surveying cytokine induction. UV-inactivated RSV induced a minute amount of the IFN-β message in mDCs but failed to induce it >6 h after stimulation, although live RSV allowed mDCs to induce incremental IFN-β >12 h post-infection (p.i.) (Fig. 2A). In contrast, the TNF-α was somehow kept to be constant >12 h in inactive RSV-stimulated mDCs (Fig. 2B). We consistently found that IFN-inducible genes were barely up-regulated by function of UV-irradiated RSV even after 6 h (data not shown) and 24 h post-stimulation (Fig. 2C). IFN-inducible genes were up-regulated only when mDCs were challenged with high doses of live RSV after 12 h. According to the ~4 h mRNA levels and 24 h ELISA results, RSV-mediated robust IFN induction is the replication-dependent event.

RSV inhibits virus–cell contact-mediated IFN-β induction

UV-inactivated RSV induced TNF-α but barely induced IFN-β in the early phase of mDCs. We asked what causes the impotent production of IFN-β in response to the external stimulation of RSV. We tested the reporter-activating abilities of RSV using the ELAM (for NF-κB) and ISRE (for IFN-β) reporter assays in HEK293 cells. Neither of the promoters was activated in response to UV-irradiated RSV at the indicated time points (Fig. 3A and B). Live RSV on the other hand prominently activated ISRE by ~24 h p.i. (Fig. 3B) and ELAM >12 h p.i. (Fig. 3A). This activation was not due to contaminating LPS since the HEK293 cells did not express TLR4 (Fig. 3A and B). The RSV replication-dependent events will markedly happen >12 h p.i..

A previous report (29) demonstrated that the RSV F protein serves as a TLR4 agonist. Thus, virus–cell contact by live and UV-irradiated RSV should extrinsically activate NF-κB via the TLR4 pathway independent of viral replication. This issue was confirmed with HEK293 cells expressing TLR4 and the stimulation period by 6 h (Fig. 3C and D). ELAM promoter activation was observed in response to live and UV-inactive RSV to a similar extent (Fig. 3C). However, virtually no ISRE activation was detected under this setting (Fig. 3D). Hence, RSV activates the IFN-β promoter in an only replication-competent fashion >24 h p.i.. There is a discrepancy between NF-κB and IFN-β promoter activation.

When HEK293 cells expressing TLR4 were stimulated with LPS and various doses of live or UV-irradiated RSV, RSV dose dependently inhibited LPS-mediated activation of the ISRE promoter (Fig. 4A) irrespective of irradiation, since the analysis was performed within 12 h i.e. before significant viral replication. To test if the inhibition was RSV (but not TLR4) specific, TLR3-expressing HEK293 cells were stimulated with polyI:C in concert with various doses of live or UV-irradiated RSV. Both live and UV-irradiated RSV dose dependently inhibited ISRE promoter activation by polyI:C in terms of TLR3 signaling (Fig. 4B). We confirmed the suppression of IFN-β induction by RSV in mDCs. IFN-β protein production by LPS or polyI:C (determined 24 h p.i.) was also dose dependently inhibited by UV-irradiated RSV in mDCs (Fig. 4C). Function-neutralizing studies were performed using polyclonal antibodies against RSV envelope proteins. We set the conditions where polyI:C induced activation of the ISRE promoter in HEK cells and this activation was partly inhibited in response to live or UV-irradiated RSV that was administered for virus–cell contact (Fig. 4D). A typical result is shown in Fig. 4(D), where the pAb against RSV abrogated RSV-dependent inhibition of ISRE promoter activation. This implies that the virus–cell contact due to a RSV-exposing factor inhibits IFN-β promoter activation in host cells. Since the RSV F protein does not activate TLR3, we used the TLR3/polyI:C system in the following inhibition experiments.

RSV G protein is surface expressed to inhibit the IFN-β pathway

The question is what factor of the RSV envelope proteins participates in inhibition of polyI:C-derived IFN-β induction. Plasmid constructs were generated with the indicated RSV envelope proteins tagged with Flag (Fig. 5A). We confirmed protein expression in HEK293 cells using SDS–PAGE and western blotting with an anti-Flag antibody (Fig. 5B). Under reducing conditions, the F, G and sG proteins were detected on the blot at their expected molecular masses (Fig. 5B). Under non-reducing conditions, all these proteins tended to form multimers. In particular, the SH and F proteins formed multimers, which were partially dissociated upon heating and reduction (Fig. 5B), consistent with a previous report (28). The F, SH and G proteins, but not sG proteins, were N-glycosylated and no high mannose was detected on these

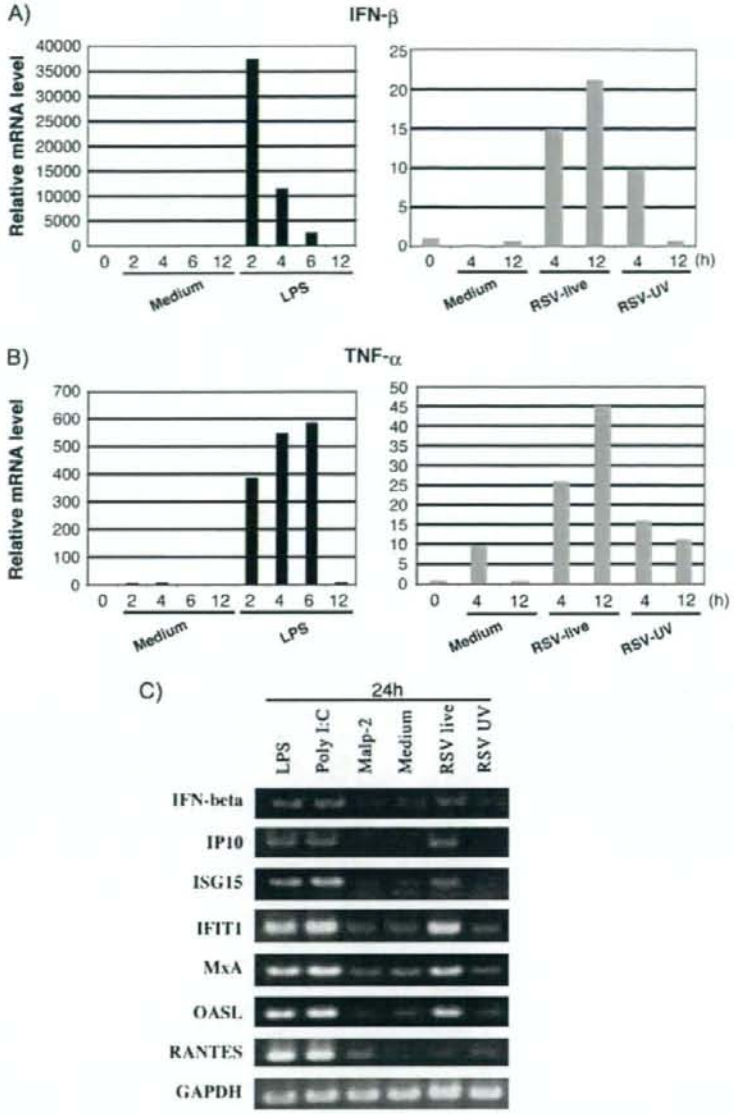

Fig. 2. Early induction of minute amounts of IFN-βthrough RSV–mDC interaction. (Panels A and B) Early induction of TNF-αand IFN-βby mDCs in response to RSV attachment. Human immature mDCs were treated with LPS (positive control), medium only (negative control) or live or UV-irradiated RSV (MOI = 0.5) as in Fig. 1(E). At indicated timed intervals, mRNA was harvested from the treated mDCs. Quantitative PCR was performed with these RNA samples pertaining to the cytokines indicated. (Panel C) Live RSV infects human mDCs and causes TLR3-independent induction of IFN-inducible genes. Human mDCs were stimulated with the reagents (indicated a top of the panel). The same lot of RSV (MOI = 0.5) as in Fig. 1(E)was used. Twenty-four hours later, mRNA levels of the indicated genes were assessed by reverse transcription–PCR. GAPDH is a control.

proteins (data not shown). Susceptibility of these proteins to glycosidases suggested that these proteins are expressed naturally on HEK293 cells. In addition, a soluble form of the G protein of 48 kDa with no high mannose or N-linked sugars was detected in the supernatant of the cells (Fig. 5C), consistent with a previous notion (33).

Cells were transfected with the indicated expression plasmid, together with TLR3-expressing plasmid and the reporter plasmids. Then, the cells were stimulated with polyI:C and after 6 h, the ISRE reporter activity was measured. G protein derivatives showed a weak ability (usually ~20%) to suppress the polyI:C-mediated ISRE reporter activity as

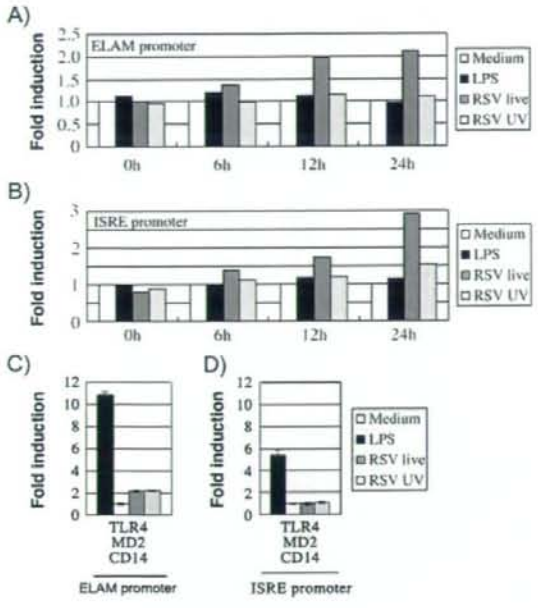

Fig. 3. Replication-dependent promoter activation by live RSV. (Panels A and B) Live but not UV-irradiated RSV activates the ELAM and ISRE promoter. HEK293 cells were transfected with pGV-E2/huELAM or pISRE-Luc and treated with the indicated stimulants as in Fig. 1(E). At timed intervals, luciferase reporter activity was determined for ELAM (A) and ISRE (B) activation. (Panels C and D) HEK293 cells with the ELAM or ISRE reporters were transfected with the plasmid set for TLR4 expression. Twenty-four hours later, cells were washed and treated with RSV (MOI = 0.5), LPS or medium. Six hours after incubation, reporter assay was performed as for ELAM (C) and ISRE (D). In either case, fold induction against medium is indicated. One of three similar experiments is shown.

compared with the vector transfectant (Fig. 6A). With the exception of the G protein, polyI:C-dependent ISRE activation was not affected by the expression of the RSV envelope proteins (Fig. 6A). The result was reproducible under the conditions where proteins were expressed to similar levels. Over-expressing RSV sG protein appears to externally inhibit the TLR3-mediated IFN-β-inducing event.

Since the sG protein maintained its inhibitory effect, we examined the ISRE inhibition by increasing doses of RSV sG protein using the TLR3 or TLR4 system. The culture supernatants from HEK293 cells transfected with the RSV sG (sGncFlag) plasmid were collected as a source of sG and used in the reporter assay. The supernatant of HEK293 cells with vector only was similarly prepared as a control. Cells were transfected with relevant plasmids for the TLR assay, and after 24 h, the cells were stimulated with LPS, polyI:C or media (presence or absence of the RSV sG protein for 6 h (Fig. 6B and C). ISRE activation by LPS–TLR4 (Fig. 6B) and polyI:C–TLR3 (Fig. 6C) were clearly inhibited by the exogenously added sG protein in a dose-dependent manner. These data suggest that it is the G protein that inhibits the TLR3/4-mediated IFN-β-inducing pathway.

Exogenously added RSV G protein suppresses IFN-β production in mDCs

It remained undetermined whether the extrinsic G protein physiologically controls mDC function. We determined IFN-β production in mDCs by stimulation with sG protein. The sG-mediated suppression of IFN production was endorsed with mDCs stimulated with polyI:C or LPS using ELISA (Fig. 7A). Finally, the purified F-protein-mediated IFN-β production was also blocked by RSV-G protein (Fig. 7B). Using the early-phase IFN-β mRNA determination assay by quantitative PCR (Fig. 2A), we checked whether exogenously added sG protein has an ability to inhibit RSV-mediated early (<2 h) induction of the IFN-β message in mDCs. The conditioned medium containing sG protein, if pre-incubated with mDCs, partially suppressed the increase of the IFN-β message by live and UV-irradiated RSV up to 4 h p.i. in mDCs (data not shown). Hence, additional sG protein can modulate mDC functions including IFN-β induction raised secondary to RSV–mDC interaction.

The sG protein selectively inhibits TICAM-1/TRIF signaling

Recent reports described the presence of TLR-independent dsRNA-mediated type I IFN-inducing pathways (38). RIG-I and MDA5 are the sensors responsible for virus RNA recognition (39). These molecules reside in the cytoplasm where they recognize dsRNA or viral RNA-specific patterns and activate IKKε and TBK1 through the adaptor MAVS (IPS-1) (18). To examine whether the sG protein could inhibit the cytoplasmic pathway, we transfected HEK293 cells with reporter plasmids together with the plasmids for the constitutively active form of RIG-I or MDA5 (ΔRIG-I or MDA5N), IPS-1, TICAM-1, IKKε or TBK-1. The IFN-inhibitory effect of the sG protein, UV-irradiated RSV and UV-irradiated MV (as a control) was assessed using the reporter assay after 6 h. The sG protein and UV-irradiated RSV inhibited ISRE activity by TICAM-1, but not by other cytoplasmic factors including RIG-I and MAVS (Fig. 8A). The TICAM-1-mediated ISRE activation was inhibited in a sG dose-dependent manner (Fig. 8B). UV-irradiated MV did not inhibit ISRE activation in terms of all the transfected constructs (Fig. 8A). IKKε/TBK-1-mediated ISRE response was not affected by the sG protein added and rather increased by stimulation with UV-irradiated RSV (data not shown), although the latter reason as yet unknown. Hence, we can conclude that the sG protein selectively inhibits the TICAM-1-signaling pathway upstream of the IRF-3 kinases, but not the RIG-I/MDA5 pathway. This issue was confirmed using TICAM-1- and MAVS-silencing HeLa cells made by the RNAi technology (M. Matsumoto and T. Seya, unpublished data).

Discussion

We demonstrated that mDCs produce only minute amounts of IFN-β in response to live and UV-irradiated RSV while mDCs induce TNF-α to mature in response to the same RSV treatment. IFN-β is poorly produced only when whole-virus particles exogenously attack for mDC infection. This situation may coincide with RSV-mediated mDC maturation which is also triggered by RSV attachment to the host cell surface.

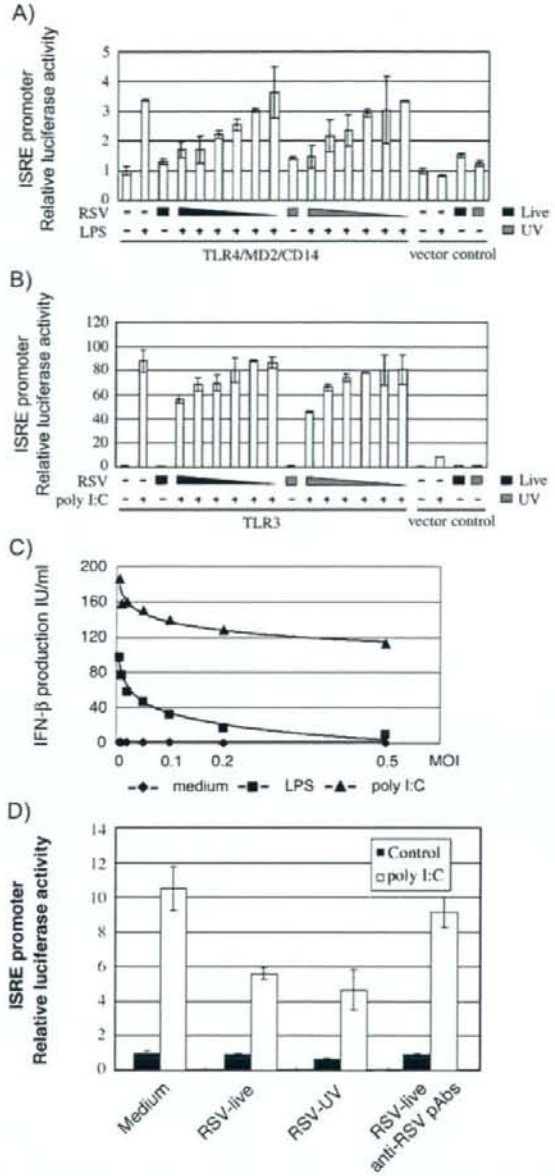

Fig. 4. RSV inhibits TLR-dependent IFN-β induction. (Panels A and B) RSV inhibits reporter activation by ISRE promoter. HEK293 cells were transfected with pISRE-Luc and phRL-TK plasmid, together with the pEFBos TLR4 plasmid sets (TLR4, MD-2 and CD14) (13) or TLR3 plasmid. Twenty-four hours later, cells were washed and treated with various doses of RSV (MOI = 0.5, 0.2, 0.1, 0.05, 0.02 and 0.01) in the presence or absence of LPS (A) or polyI:C (B). Six hours after incubation, cell lysates were subjected to the assay for the dual reporters (13). Fold induction against the medium control is indicated. (Panel C) Immature mDCs were treated with UV-irradiated RSV (MOI indicated) together with LPS or polyI:C. Twenty-four hours later, culture supernatants were collected and the levels of IFN-β measured by ELISA. (Panel D) RSV-mediated inhibition of ISRE promoter activation is abrogated by the addition of pAbs against RSV. HEK293 cells with TLR3 and ISRE promoter were treated with polyI:C (medium) and live (RSV-live) or inactive RSV (RSV-UV) (as in B). Under the conditions where the RSV-mediated inhibition was observed, pAbs against RSV were added to the cells (RSV-live, anti-RSV pAbs). Six hours after incubation, cell lysates were subjected to the assay for the dual reporters.

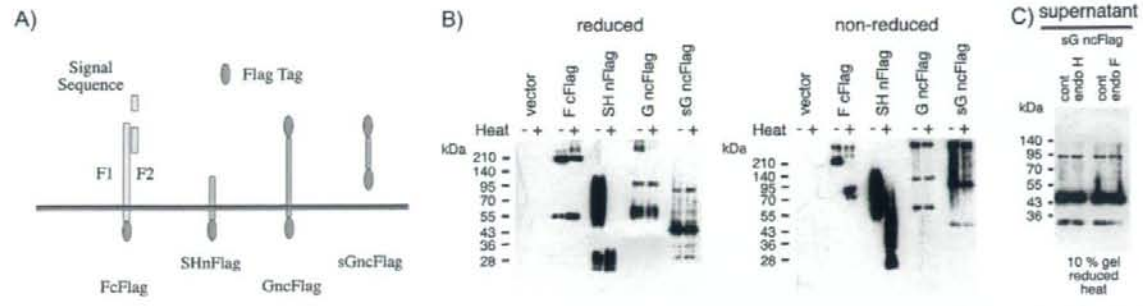

Fig. 5. Detection of the RSV envelope proteins expressed on HEK293 cells. (Panel A) Scheme of the Flag-tagged RSV proteins. Predicted proteins are shown based on the constructs we prepared. F, SH, G and sG are RSV envelope proteins. Flag-labeled (N-terminal, n and/or C-terminal, c) is indicated. Elliptic circles indicate the Flag-tag. FcFlag, C-terminal-flagged F protein; SHnFlag, N-terminal-flagged SH protein; GncFlag, both N- and C-terminal-flagged G protein; sGncFlag, N- and C-terminal-flagged secreted G protein. (Panel B) Immunoblotting analysis of RSV envelope proteins in HEK293 cells. Cells were transfected with the plasmids encoding the RSV envelope proteins tagged with Flag (see A). Twenty-four hours later, cell lysates were immunoprecipitated with anti-Flag antibody and the proteins were resolved on SDS–PAGE (10% gel) under reducing (left panel) or non-reducing conditions (right panel). After protein blotting onto a sheet, blots were probed with anti-Flag pAb. (Panel C) Glycosylation of RSV proteins liberated from HEK cells. The supernatants of the sGncFlag-transfected HEK293 cells in (B) were treated with endoglycosidase H (endo H) or endoglycosidase F (endo F) and analyzed on SDS–PAGE followed by immunoblotting. The conditions of the analyzed samples are shown in the panel.

We found RSV inducing minimal IFN-β through virion–cell attachment (usually taking <4 h p.i.) and then inducing robust IFN-β after cytoplasmic replication (>12 h p.i.). The F protein should be an effector for the RSV-mediated IFN-β induction, but somehow the IFN-β induction tends to be diminished in RSV–host cell interaction. We searched for the factor negatively regulating IFN-β induction in host HEK293 cells using UV-inactive RSV and found that attachment of RSV envelope proteins to host cells causes down-regulation of IFN-β. Finally, the G protein of RSV is the factor for the inhibition of IFN-β promoter activation: even by the stimulation with polyI:C or LPS, bystander inhibition happens by function of the soluble form of the G protein (sG). Addition of the sG protein to the culture of mDCs allows the suppression of polyI:C- or LPS-mediated IFN-β production. Ultimately, here we disclose a novel function of the RSV G protein in the regulation of host cell IFN response.

Using *in vitro* analysis, we found that the RSV F protein-mediated IFN induction (30) is neutralized by the RSV G protein, which selectively modulates the TICAM-1 pathway, i.e. the preferential activation of IRF-3 and the IFN-β promoter in myeloid DCs. The G protein can inhibit both TLR3 and TLR4 to suppress IFN-β induction, supporting the target TICAM-1. Studies using reporter analysis, ELISA with mDCs and gene-silencing analysis of MAVS and TICAM-1 using RNAi (M. Matsumoto and T. Seya, unpublished data) all supported the G protein function in the TICAM-1 pathway.

How the G protein modulates the TICAM-1-mediated IFN-inducing function remains as a tantalizing point in this story. A possible molecular mechanism is that the G protein is produced after replication and a putative receptor for the G protein delivers a negative signal to the TICAM-1 pathway. This G protein receptor may exist in the cytoplasmic compartment or on cell surface and link the TICAM-1 pathway in the cytoplasm. This hypothesis may be related to the fact that a defective recombinant virus lacking the sG protein decreases the virus pathogenicity due to the induction of antiviral immunity (40). In addition, how dsRNA stimulation activates TICAM-1 is getting clear in a molecular level (41). Furthermore, a recent report (42) suggested that the TIR-containing adaptor SARM exhibits a regulatory function toward TICAM-1. Further studies are required to clarify the mode for TICAM-1 inhibition by extrinsic G proteins.

Since IFN-inducible genes are significantly up-regulated in mDCs in response to live RSV after 24 h p.i. (Fig. 2C), the initial trigger of IFN induction by live RSV may be too weak to suppress RSV replication, so that the infected mDCs elicit following replication-mediated response. In fact, importance of 'revving up' activation of IFN-β for amplifiable IFN-α/β response has been proposed in a recent review (43). RIG-I and MDA5 are preferentially responsible for the replication-dependent antiviral event in response to live viruses, which is evident in the airway epithelial cells (6). Since RIG-I and MDA5 are IFN-inducible proteins, an initial trigger of IFN-β also critically causes their induction in virus-attached cells. We surmise the importance of F protein-mediated TLR4 signal in an early response of cells to RSV. Blocking of the F protein function by G proteins may be crucial for silencing the IFN-inducing response and for the virus side facilitating RSV infection. Indeed, immature mDCs secrete TNF-α and mature in a similar manner in response to both live and dead RSV, possibly reflecting minute participation of type I IFN in the RSV-mediated maturation phenotype of mDCs.

The difference in outcome between TLR and RIG-I/MDA5 signaling is an intriguing question. TLR3 senses viral RNA outside the cytoplasm and RIG-I/MDA5 sense it inside the cytoplasm. RIG-I/MDA5 and TLR3 recruit different adaptors, IPS-1 and TICAM-1, respectively. Although TICAM-1 and IPS-1 interact partly with TANK family proteins (10, 44), only the TICAM-1 pathway is reported to elicit potencies to activate CTL and NK cells in mDCs (11, 12). Our premise is that viral RNA replication inside the cytoplasm and extrinsic dsRNA stimulation lead to differential mDC driving. Selective inhibition

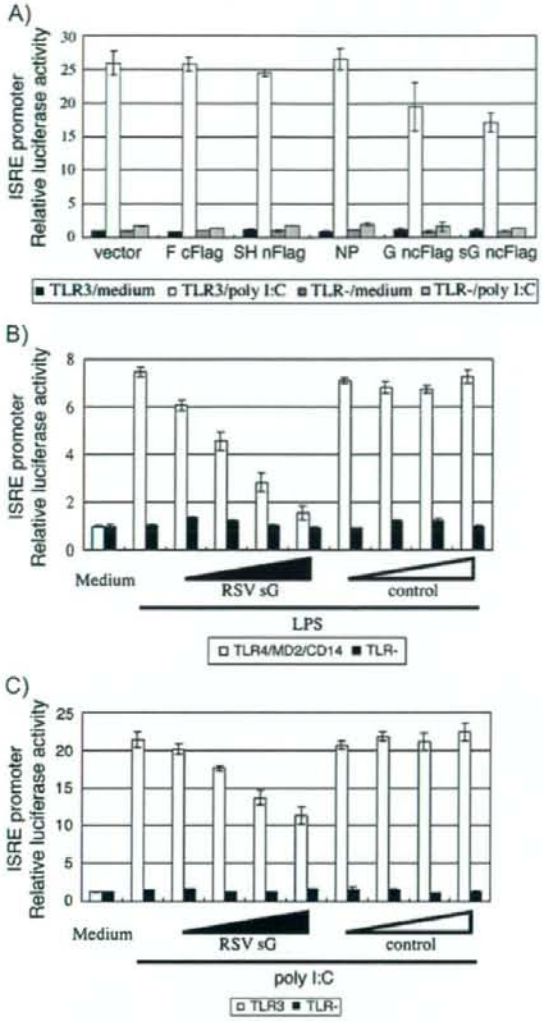

Fig. 6. RSV G protein inhibits activation of the ISRE promoter. (Panel A) RSV G protein inhibits ISRE activation by TLR3. HEK293 cells were transfected simultaneously with pISRE-Luc, phRL-TK, pEFBos TLR3 and indicated plasmids encoding RSV proteins. Twenty-four hours later, cells were incubated with 10 μg ml^{-1} of polyI:C or buffer only. After 6 h, dual-luciferase reporters were assayed as in Fig. 4(A). (Panel B and C) sG protein inhibits ISRE activation by LPS or polyI:C. HEK293 cells expressing TLR4/MD-2/CD14 or TLR3 were prepared and then the ligand stimulation was added to the cells in the medium containing RSV sG. HEK293 cells were transfected with pISRE-Luc, phRL-TK and pEFBos TLR4 expression plasmids or TLR3 plasmid. Twenty-four hours later, cells were stimulated with 100 ng ml^{-1} of LPS (B) or 10 μg ml^{-1} of polyI:C (C) under various doses of RSV sG (1/5, 1/10, 1/20 and 1/40 volumes of medium). The culture supernatant from the empty vector-transfected cells was used as a control. After 6 h incubation, luciferase reporter activity was measured as in Fig. 4(A). The figures are representative results of multiple trials.

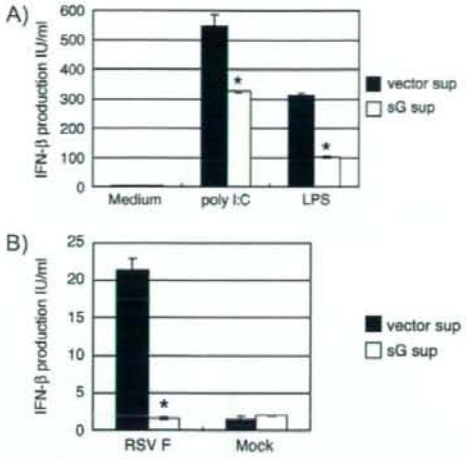

Fig. 7. RSV sG protein inhibits IFN-β production by mDCs stimulated with polyI:C or RSV F protein. (Panel A) sG protein inhibits polyI:C-inducing IFN-β production in human mDCs. mDCs were prepared as in Fig. 1. Cells were stimulated with polyI:C in the presence of the sG protein-containing or control medium. Twenty-four hours later, the supernatants were harvested to measure the IFN-β content. LPS was used as control as in Fig. 2(D). (Panel B) Purified F protein allows mDCs to produce IFN-β, which is inhibited by sG. Immature mDCs were stimulated with the purified F protein (1 μg) in the presence or absence of the sG-containing medium. Twenty hours later, the IFN-β levels released in the supernatant of mDCs were determined by ELISA.

of the TICAM-1 pathway may benefit RSV survival and happen to suppress mDC-derived cellular immune responses. Severe repetitive infection by RSV occurring in children and being referred to insufficient mDC maturation, may be partly due to this extrinsic mDC regulation by RSV proteins.

The question is whether the early IFN induction via RSV-attached host cells is physiologically significant in mDCs. A number of RSV studies have suggested that TLR3 is implicated in the immune response of epithelial cells. IL-8, RANTES, TNF-α and IL-6 are up-regulated secondary to RSV infection (45–47). In addition, IFN-inducible genes, including *TLR3* and *PKR*, are up-regulated (5). These findings were reported before the molecular identity of RIG-I/MDA5 was completed and were based on the assumption that the source of dsRNA was from RSV RNA released from cells undergoing infection-induced apoptosis. It is still unclear whether the virus–cell attachment-mediated TICAM-1 blocking earlier and more significantly participates in initial IFN induction than the intrinsic cytoplasmic IFN-inducing pathway. However, in RSV infection, this G protein-mediated TICAM-1 blocking would be crucial since RSV possesses the TLR4 ligand F protein. The question is whether these findings are adaptable to human patients with RSV infection. Further analysis will be required about what happens in mDCs and acquired immunity once replication-derived viral RNA products are generated in patients' body (8, 9).

Regarding viral aspects, a recent report suggested that the G cysteine-rich region of the RSV sG protein inhibits production of NF-κB-inducible inflammatory cytokines through TLR4 (48). Since MyD88 is not a target of the RSV G

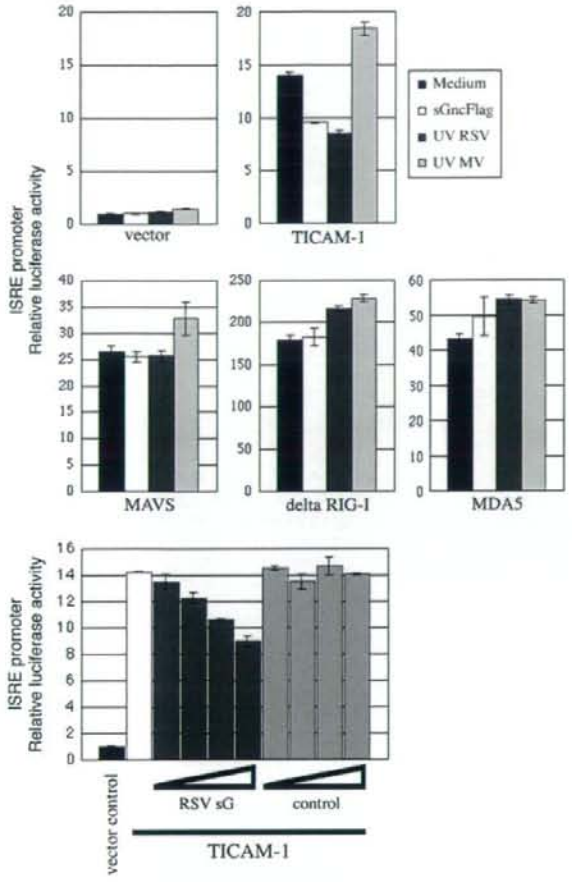

Fig. 8. The sG protein inhibits the TICAM-1 pathway. (Panel A) The sG protein blocks TICAM-1-mediated ISRE promoter activation. HEK293 cells were treated with a control medium or medium containing sG along with control dead RSV or MV and transfected with pISRE-Luc, phRL-TK and the plasmids expressing for the indicated proteins. Six hours later, cells were washed, lysed with lysis buffer and the reporter assay was performed as in Fig. 4(A). (Panel B) The sG protein dose dependently inhibits the TICAM-1 pathway. HEK293 cells were transfected with the TICAM-1 plasmid, and the TICAM-1-mediated ISRE promoter activation was monitored in the presence of variable amounts of the RSV sG-containing medium (1/5, 1/10, 1/20 and 1/40 volumes of medium). The culture supernatant from the empty vector-transfected cells was used as a control.

proteins in NF-κB activation (data not shown), the G protein can distinguish between MyD88 and TICAM-1 as the molecular target. Besides the RSV F protein, many viral envelope proteins are known to act as ligands for TLR2 or TLR4. In general, many viral proteins reportedly inhibit the JAK/STAT pathway and IRF-3 activation. NS3/4A of HCV inactivates IPS-1 and TICAM-1 by proteolysis (49). Vaccinia virus proteins also target TLR adaptor proteins (50). RSV NS1 and NS2 are simultaneously generated with viral RNA in the cytoplasm. These proteins act as inhibitors for IFN-α/β signaling after replication (26, 27). Here, we add to these findings a line of evidence that the RSV G protein is a negative regulator for the TLR3/4-mediated TICAM-1 pathway.

Funding

CREST and Innovation; Japan Science and Technology Corporation; Program of Founding Research Centers for Emerging and Reemerging Infectious Diseases; MEXT; Ministry of Education, Science, and Culture (Specified Project for Advanced Research); Ministry of Health, Labor and Welfare of Japan.

Acknowledgements

We are grateful to A. Ishii and A. Matsuo in our laboratory for their critical discussions. Thanks are also due to K. Imai (Wakayama Prefectural Center, Wakayama) for providing us with RSV, to T. Taniguchi (University of Tokyo, Tokyo), T. Fujita (Kyoto University, Kyoto), K. Miyake (University of Tokyo, Tokyo), M. Nakanishi (The Nagoya City University, Nagoya) and T. Maniatis (Harvard University, Boston, MA, USA) for providing their plasmids. Support by Takeda Science Foundation and NorthTec Foundation are gratefully acknowledged.

Abbreviations

DC	dendritic cell
dsRNA	double-stranded RNA
F protein	fusion glycoprotein
G protein	G glycoprotein
IKKε	IκB kinase-related kinase ε
IPS-1	IFN-β promoter stimulator 1
IRF	IFN-regulatory factor
MALP-2	macrophage-activating lipopeptide-2
MAVS	mitochondria antiviral signaling
MDA5	melanoma differentiation-associated gene 5
mDC	monocyte-derived dendritic cell
MOI	multiplicity of infection
MV	measles virus
NF-κB	nuclear factor-κB
p.i.	post-infection
RIG-I	retinoic acid-inducible gene I
RSV	respiratory syncytial virus
sG	soluble G
TBK1	TANK-binding kinase 1
TIR	Toll–IL-1R
TLR	Toll-like receptor
TNF-α	tumor necrosis factor-α

References

1 Ogra, P. L. 2004. Respiratory syncytial virus: the virus, the disease and the immune response. *Paediatr. Respir. Rev.* 5:119.

2 Steinman, R. M. and Hemmi, H. 2006. Dendritic cells: translating innate to adaptive immunity. *Curr. Top. Microbiol. Immunol.* 311:17.

3 Srikiatkhachorn, A. and Braciale, T. J. 1997. Virus-specific CD8+ T lymphocytes downregulate T helper cell type 2 cytokine secretion and pulmonary eosinophilia during experimental murine respiratory syncytial virus infection. *J. Exp. Med.* 186:421.

4 Creagh, E. M. and O'Neill, L. A. 2006. TLRs, NLRs and RLRs: a trinity of pathogen sensors that co-operate in innate immunity. *Trends Immunol.* 27:352.

5 Groskreutz, D. J., Monick, M. M., Powers, L. S., Yarovinsky, T. O., Look, D. C. and Hunninghake, G. W. 2006. Respiratory syncytial virus induces TLR3 protein and protein kinase R, leading to increased double-stranded RNA responsiveness in airway epithelial cells. *J. Immunol.* 176:1733.

6 Liu, P., Jamaluddin, M., Li, K., Garofalo, R., Casola, A. and Brasier, A. 2007. Retinoic acid inducible gene-I mediates early anti-viral